

MULTIYEAR OBSERVATIONS OF THE TROPICAL ATLANTIC ATMOSPHERE

Multidisciplinary Applications of the NOAA Aerosols and Ocean Science Expeditions

BY NICHOLAS R. NALLI, EVERETTE JOSEPH, VERNON R. MORRIS, CHRISTOPHER D. BARNET,
WALTER W. WOLF, DANIEL WOLFE, PETER J. MINNETT, MALGORZATA SZCZODRAK, MIGUEL A. IZAGUIRRE,
RICK LUMPKIN, HUA XIE, ALEXANDER SMIRNOV, THOMAS S. KING, AND JENNIFER WEI

The Aerosols and Ocean Science Expeditions (AEROSE) have collected an unprecedented set of atmospheric data from the tropical Atlantic Ocean, sampling a broad range of important regional meteorological phenomena.

The tropical Atlantic Ocean is a region of significant meteorological and oceanographic interest in terms of atmospheric chemistry and mesoscale-to-synoptic dynamical and thermodynamical processes. Nonmaritime air masses from the African continent advect out over the Atlantic within easterly winds and waves, significantly impacting the meteorology and climate dynamics downstream into the Western Hemisphere. In particular, large-scale

outflows of Saharan dust extend well out over the Atlantic within persistent stable layers of dry and warm air collectively referred to as the Saharan air layer (SAL) (e.g., Carlson and Prospero 1972; Zhang and Pennington 2004; Dunion and Velden 2004; Nalli et al. 2005). Additionally, finer mode smoke aerosols from biomass burning to the south also advect over the Atlantic, which in turn has an impact on the regional atmospheric chemistry.

AFFILIATIONS: NALLI, KING, AND WEI—Dell Services Federal Government, Inc., and NOAA/NESDIS Center for Satellite Applications and Research (STAR), Camp Springs, Maryland; JOSEPH AND MORRIS—NOAA Center for Atmospheric Sciences, Howard University, Washington, D.C.; BARNET AND WOLF—NOAA/NESDIS Center for Satellite Applications and Research, Camp Springs, Maryland; WOLFE—NOAA Earth System Research Laboratory, Boulder, Colorado; MINNETT, SZCZODRAK, AND IZAGUIRRE—Rosenstiel School of Marine and Atmospheric Science, University of Miami, Miami, Florida; LUMPKIN—NOAA/OAR Atlantic Oceanographic and Meteorological Laboratory, Miami, Florida; XIE—I. M. Systems Group, NOAA/NESDIS/STAR, Camp Springs, Maryland; SMIRNOV—

Sigma Space Corporation, NASA Goddard Space Flight Center, Greenbelt, Maryland

CORRESPONDING AUTHOR: N. R. Nalli, NOAA/NESDIS/STAR, Airmen Memorial Bldg Ste 204, 5211 Auth Road, Camp Springs, MD 20746-4304

E-mail: nick.nalli@noaa.gov

The abstract for this article can be found in this issue, following the table of contents.

DOI:10.1175/2011BAMS2997.1

In final form 11 January 2011
©2011 American Meteorological Society

Acquiring synoptic-scale observations over oceans using conventional in situ methods is a difficult and impractical task, typically leaving marine atmospheres severely undersampled, an undesirable situation given that oceans play a major role in atmospheric forcing. An obvious solution would be the use of remotely sensed data from visible, infrared (IR), and microwave (MW) sensors onboard geosynchronous and sun-synchronous environmental satellites. However, the unusual nature of the African continental influence over the otherwise maritime environment of the Atlantic presents a challenge for satellite retrievals. Among other things, dust aerosols introduce a systematic perturbation to satellite-measured IR spectral radiances (mostly through absorption and reemission) that can negatively impact geophysical parameter retrievals (e.g., Stowe and Fleming 1980; Nalli and Stowe 2002; Weaver et al. 2003; Zhang and Zhang 2008). To date, the impact of dust aerosols on satellite retrievals has not been fully accounted for in operational products. Furthermore, the SAL itself is defined by very sharp vertical temperature and moisture gradients that are difficult to resolve in the vertical using passive sounders (cf. Nalli et al. 2005, 2006).

THE AEROSOLS AND OCEAN SCIENCE EXPEDITIONS. To address these topics related to the measurement of African dust and smoke phenomena (e.g., as addressed by Kahn et al. 2004) over the tropical Atlantic, the U.S. National Oceanic and Atmospheric Administration (NOAA), in collaboration with the Howard University NOAA Center for Atmospheric Sciences (NCAS), has supported a series of multidisciplinary, trans-Atlantic Aerosols and Ocean Science Expeditions (AEROSE) onboard the blue-water NOAA ship *Ronald H. Brown* to acquire simultaneous in situ and remotely sensed marine data during intensive observing periods. Following the first AEROSE in 2004, a number of AEROSE follow-up campaigns have been conducted as a synergistic component of the NOAA Prediction and Research Moored Array in the Tropical Atlantic (PIRATA) Northeast Extension (PNE) project (Bourlès et al. 2008). As a complement to the PNE cruises, the multiyear AEROSE program has grown to become one of the most extensive collections of in situ measurements over the tropical Atlantic Ocean.

The three central scientific questions addressed by AEROSE are described in Morris et al. (2006). This paper summarizes the campaigns with an eye toward

the third objective, namely to assess the capability of environmental satellite observing systems for detecting and resolving processes of interest pertaining to Saharan and sub-Saharan trans-Atlantic outflows, including the evolution of dust and smoke aerosol distributions during transport, and the impact of these outflows on the regional atmosphere and ocean, with increased understanding of these phenomena being the primary objective. In particular, we elaborate on data of value for validation of advanced satellite sounders and demonstrate their utility for observing synoptic to mesoscale phenomena like those mentioned above; it is under these “hard” but meteorologically interesting circumstances that satellites can potentially have the greatest positive impact on numerical weather prediction (NWP).

AEROSE FOR SATELLITE SOUNDER VALIDATION.

Of particular interest for this objective are atmospheric profile data obtained via dedicated rawinsondes and ozonesondes, described below in more detail. These provide independent correlative data necessary for pre-launch phase validation of environmental data records (EDRs) derived from the NOAA Joint Polar Satellite System (JPSS) and Preparatory Project (NPP) (hereafter jointly called JPSS) Cross-track Infrared Microwave Sounding Suite (CrIMSS)¹ and the NOAA Geostationary Operational Environmental Satellite R series (GOES-R) Advanced Baseline Imager (ABI) [see Schmit et al. (2005) for details on ABI]. Validation in the prelaunch phase is facilitated through the development of “proxy datasets” (i.e., sensor data approximated from existing satellite systems with similar specifications). Specifically, the planned low Earth orbit (LEO) CrIMSS sounding system will be designed to operate in much the same manner (in terms of scanning, cloud-clearing methodology, and spectral/spatial resolution and coverage) as the Infrared Atmospheric Sounding Interferometer (IASI) and Advanced Microwave Sounding Unit (AMSU-A) system onboard *MetOp-A* [see Cayla (1993) for details on IASI], as well as the Atmospheric Infrared Sounder (AIRS)–AMSU system onboard Earth Observing System (EOS) *Aqua* [see Chahine et al. (2006) for details on AIRS] in the NASA A-Train. Similarly, the GOES-R ABI will have spectral channels, temporal resolution, and view geometry (e.g., Schmit et al. 2005) very close to the Spinning Enhanced Visible and Infrared Imager (SEVIRI) onboard Meteosat in geosynchronous Earth

¹ The CrIMSS consists of two passive sensors: the Cross Track Infrared Sounder (CrIS), a high-resolution IR Fourier transform spectrometer (FTS), and the Advanced Technology Microwave Sounder (ATMS).

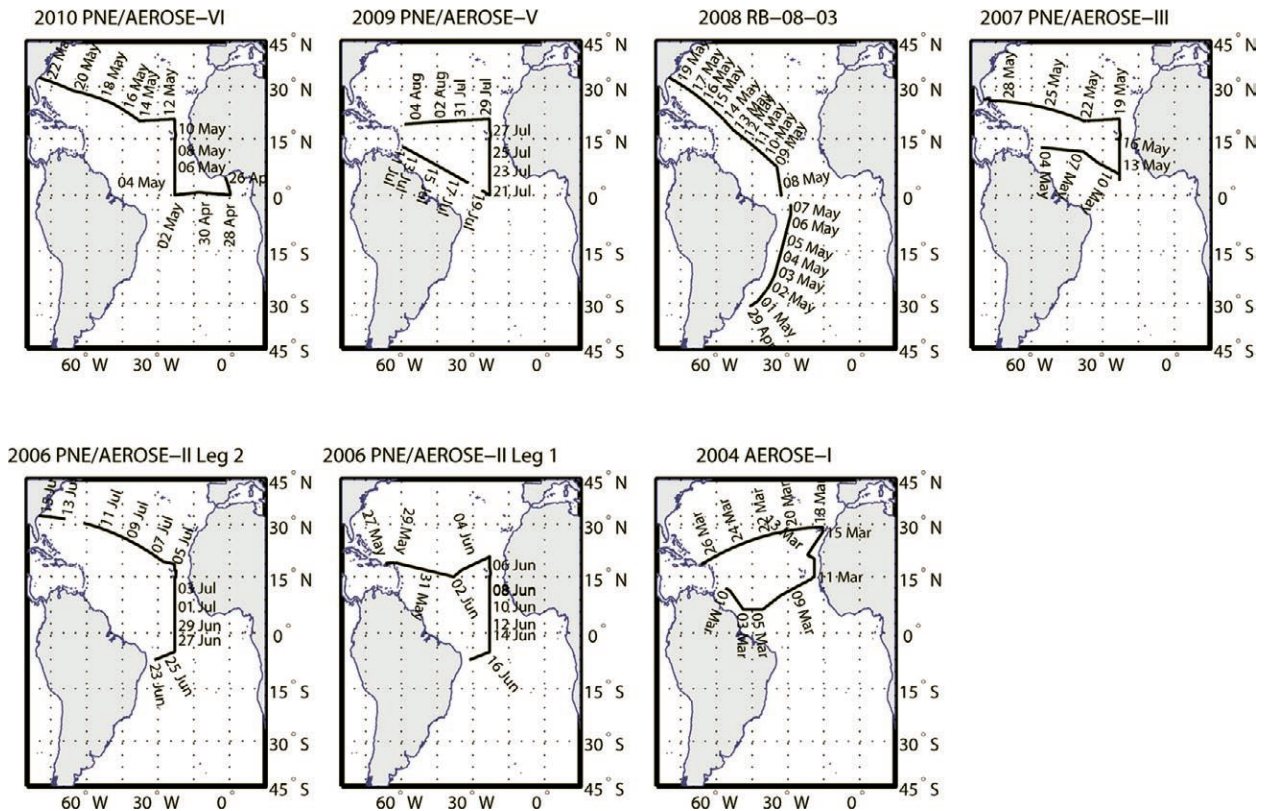


FIG. 1. AEROSE cruise tracks and dates. Areas of missing track lines are the result of data blackouts imposed on the *Ronald H. Brown* within exclusive economic zones (EEZs) without prior clearance (e.g., Brazilian). Map projections are cylindrical equal area.

orbit (GEO) [see Schmetz et al. (2002) for details on Meteosat].

Measurements over the open ocean are particularly advantageous for calibration/validation (e.g., Hagan and Minnett 2003) given that the sea surface radiative properties (i.e., emission skin temperature and spectral emissivity/reflectivity) are well characterized and uniform (e.g., Smith et al. 1996; Nalli et al. 2006, 2008a), thus allowing these state parameters to be specified accurately. It is over open oceans, which constitute $\approx 70\%$ of Earth's surface area, where satellite data are known to make their biggest impact on NWP, as demonstrated by consistently greater impact in the Southern Hemisphere (SH) (e.g., Le Marshall et al. 2006). Furthermore, the multi-institutional and multidisciplinary nature of PNE/AEROSE allows for research synergy whereby all collaborators benefit by gaining access to the various data, the broader science community (including actual and potential users of satellite products) is engaged, and NOAA's allocation

of ship time onboard the *Ronald H. Brown* for PNE/AEROSE cruises is fully optimized.²

OVERVIEW OF AEROSE CAMPAIGNS. As mentioned above, the geographic domain of AEROSE has been the Atlantic Ocean, primarily the tropical North Atlantic. Figure 1 shows the cruise tracks and times for the AEROSE domain to date; as can be seen, there is excellent coverage over most of the domain. A brief summary of each cruise follows below.

Cruise summaries. AEROSE-I, conducted during March 2004, was the main mission onboard the *Ronald H. Brown*, the details of which have been documented in earlier papers (Nalli et al. 2005, 2006; Morris et al. 2006). The AEROSE mission objectives continued jointly as part the 2006 PNE/AEROSE-II cruise, initiated in conjunction with the 2006 African Monsoon Multidisciplinary Analysis (AMMA) [see Redelsperger et al. (2006) for details on AMMA] and

² It is an undeniable and oft understated cost benefit to have a synergistic ocean/atmosphere campaign fully utilize the ship resource. For example, PNE/AEROSE does not waste fuel and resources during "transit legs" to buoys—it is precisely during these legs that some of the most valuable AEROSE data is collected.

AEROSE AND EDUCATIONAL PARTNERSHIPS

The AEROSE campaigns form an essential component of the Howard University NOAA Center for Atmospheric Sciences (NCAS) research and education program. NCAS is a NOAA Cooperative Science Center funded by the NOAA Office of Education's Educational Partnership Program (Morris et al. 2007) aligned with the National Environmental Satellite Data and Information Service, the National Weather Service, and the Office of Oceanic and Atmospheric Research [for more information, see Robinson et al. (2008)]. AEROSE has sought an interdisciplinary approach by involving team members not only from atmospheric and oceanographic sciences but also from biology, environmental, and health sciences.

In addition to this, AEROSE has explicitly sought to provide unique, hands-on field experience for graduate and undergraduate students working alongside NOAA scientists and NCAS faculty aboard a state-of-the-art NOAA research vessel. Students from partnering institutions within NCAS [e.g., University of Puerto Rico Mayagüez (UPRM)] are routine participants in the AEROSE campaigns. Students from other cooperative science centers [namely CREST and Interdisciplinary Scientific Environmental Technology (ISET)] have also participated. To date, several graduate students from these programs have graduated or are currently working with AEROSE-related thesis topics. Each campaign offers once-in-a-lifetime opportunities by exposing students to the various challenges of data collection, real-world problem solving, teamwork, safety, and scientific camaraderie at sea.* On average, approximately eight students participate in each campaign (not including PNE participants), roughly evenly distributed between male (47%) and female (53%). Many of these students are recruited from

*One such experience by 2010 student M. Oyola was recently featured in the AMS blog, *The Front Page* (<http://blog.ametsoc.org/uncategorized/not-seasick-science-smitten/>).

minority-serving institutions serving to increase the presence and participation of African American, Hispanic, and Native American students/scientists/faculty in the atmospheric and oceanic sciences (Robinson et al. 2007; Morris et al. 2010). By race/ethnicity we have had approximately 29% African American, 47% Hispanic, 6% Caucasian Americans, and 18% international (from Benin, Nigeria, Mexico, Columbia, and Spain).

We have specifically designed and implemented several educational activities to ensure student development and outreach during each AEROSE cruise. Specific elements include the following:

Nightly weather briefings. Participating students are charged with developing and delivering weather briefings in nightly scientific meetings to assist in planning and execution of underway deployments of soundings, sampling, and other relevant measurements.



FIG. S1: Howard University Prof. E. Joseph giving an evening science seminar in the Main Lab during the 2010 AEROSE-VI campaign.



FIG. S2: Howard University graduate student A. Flores giving instruction to students on the operation of the Microtops sunphotometer during the 2009 AEROSE-V.

Scientific seminars. AEROSE sponsors an evening seminar series that features the research of participating professional scientists and faculty (Fig. S1). These seminars are open to the entire ship and are often attended by officers, crew members, and PNE investigators.

Student projects. Each participating student is assigned a research project in support of the mission. During the mission they deploy and maintain sensors and conduct quality control and preliminary analysis of collected data (Figs. S2 and S3). They are then required to give a summary on what they learned and the specific work they accomplished during the campaign. These presentations will often include basic overviews on instrumentation, data collection, and research findings.

Shoreside seminars. When scheduling permits, seminars are arranged at universities and agencies in the various ports of call. A recent example includes one of the coauthors (V. Morris) delivering a seminar to a summer program hosted by the University of the West Indies at Cave Hill, Barbados (Fig. S4). Similar activities have been conducted with universities and scientific researchers in the Canary Islands, Argentina, Puerto Rico, Senegal, and Ghana.

Web access. AEROSE has used the World Wide Web for students and the community at large to post questions, follow blogs from scientists aboard the ship, and interact with the AEROSE participants. Beginning in 2009, a Facebook group page was created to streamline this endeavor.

Scientific tours. AEROSE scientists and grad students participate in ship tours arranged for local school groups and university guests (Fig. S5).



FIG. S3: Morehouse College student M. Fuller launching RS92 rawinsonde 30 min prior to LEO satellite sounder overpass during the 2010 AEROSE-VI.



FIG. S4: Howard University Prof. V. Morris (center front) with students at the University of the West Indies at Cave Hill, Barbados, prior to the start of the 2009 AEROSE-V campaign.



FIG. S5: Howard University graduate student C. Stearns giving an overview of the EN-SCI ECC ozonesonde to a student tour onboard the *Ronald H. Brown* while in Montevideo, Uruguay, just prior to the 2008 AEROSE Interhemispheric Transit.

successfully carried out in two 4-week legs during June–July 2006 (Morris et al. 2006; Nalli et al. 2008a). The success of the 2006 campaign firmly established the PNE–AEROSE collaboration, and thus the PNE/AEROSE-III cruise followed in May 2007. The fourth PNE/AEROSE campaign was scheduled for April–May 2008 (Cruise RB-08-03), with the port of origin being in Montevideo, Uruguay. The final cruise track consisted of a unique interhemispheric transit³ resembling the Aerosols99 cruise during January–February 1999 from Norfolk, Virginia to Capetown, South Africa [for more details on Aerosols99, see Thompson et al. (2000), Bates et al. (2001), and Voss et al. (2001)]. The fifth and sixth campaigns, PNE/AEROSE-V and AEROSE-VI, were successfully executed as planned during July–August 2009 and late April–May 2010, respectively. Both of these latter campaigns were somewhat unique in terms of sampling, the first occurring somewhat later in the summer (coinciding with the seasonal climatological peak of dust outflows) and the latter initiating out of Ghana, Africa, allowing for unique sampling of the Gulf of Guinea.

Data overview. Through joint collaborations (see the acknowledgments), the AEROSE campaigns have all been equipped with balloon-borne radiosondes and ozonesondes funded primarily to support the satellite validation objectives (discussed in Nalli et al. 2006), with launch times mostly coordinated to coincide with twice-daily LEO sounder overpasses (referred to as “dedicated sondes”—launch times are scheduled ≈ 0.5 h prior to a predicted overpass time at the ship location), namely the A-Train *Aqua* AIRS/AMSU and, starting in 2007, the MetOp IASI/AMSU. The AEROSE radiosonde observations (RAOBs) are obtained from Vaisala rawinsondes (RS92-SGP and, in 2004, RS80-H and RS90) and include thermodynamic soundings of pressure, temperature, and relative humidity (RH) (collectively “PTU”). The Vaisala sondes also measure wind vectors (i.e., speed and direction) via a Global Positioning System (GPS), thus providing wind profiles,⁴ with the RS92 sondes also providing geometric heights of measurement levels. Because GPS heights are obtained independent of the pressure sensor, they may be of value for validation of satellite-derived pressure (a CrIMSS EDR) as

a function of altitude levels. The AEROSE RAOBs from the 2004 and 2008–10 campaigns have not been assimilated into numerical forecast models, thereby ensuring truly independent correlative data for those years.⁵ In addition to the RS92 PTU-wind soundings, EN-SCI Corporation electrochemical concentration cell (ECC) ozonesondes are interfaced (OIF92 interface) approximately once per day (launched ≈ 1.0 h prior to the predicted overpass time) to provide ozone profiles up through the lower stratosphere.

Figure 2 charts the geographic locations and dates of the rawinsonde and ozonesonde launches. It can be seen that AEROSE has attained multiple latitudinal and longitudinal Atlantic transects with RAOB frequencies that enable space–time cross-sectional analyses of temperature, moisture, winds, and ozone as a function of altitude and ship coordinate. These profile cross sections are presented and overviewed in section 3. In addition to the RAOB data, a suite of other ship-based sensors are deployed during each AEROSE campaign as briefly summarized below.

Marine Atmospheric Emitted Radiance Interferometers (M-AERIs) [see Minnett et al. (2001) for full details on M-AERI] provide measurements of well-calibrated, high-resolution atmospheric and oceanic radiance spectra (Minnett et al. 2001). From the M-AERI spectra, a number of critical geophysical state parameters can be derived, including high-accuracy radiometric sea surface skin temperature, IR spectral emissivity (e.g., Smith et al. 1996; Hanafin and Minnett 2005; Nalli et al. 2008a), and retrievals of boundary layer temperature and water vapor (e.g., Feltz et al. 1998; Szczo drak et al. 2007).

Microtops handheld sunphotometers provide multichannel observations of solar-spectrum aerosol optical depth (AOD), thereby providing a measure of column-integrated aerosols at the ship’s location. Starting in 2009, AEROSE has collaborated with the NASA Goddard Space Flight Center (GSFC) Maritime Aerosol Network (MAN) to apply the MAN methodology for maritime (ship-based) Microtops observations described in Smirnov et al. (2009), including sensor calibration, raw data processing, and quality assurance (QA); AEROSE Microtops data prior to 2009 have been subsequently reprocessed using the MAN methodology.

³ Because of serious mechanical problems onboard the *Ronald H. Brown*, brought on by a grueling yearly cruise schedule, departure was delayed by over two weeks. The original cruise plan was thus severely descope d to assume a more direct track back to the United States (instead of eastward to 23°W), thereby entirely canceling the PNE component of the mission.

⁴ With the exception of the RS90 sondes launched near the end of the 2004 AEROSE-I.

⁵ During the 2006 and 2007 campaigns some sondes were uploaded into the Global Telecommunications System for numerical forecast model assimilation in cooperation with the AMMA program.

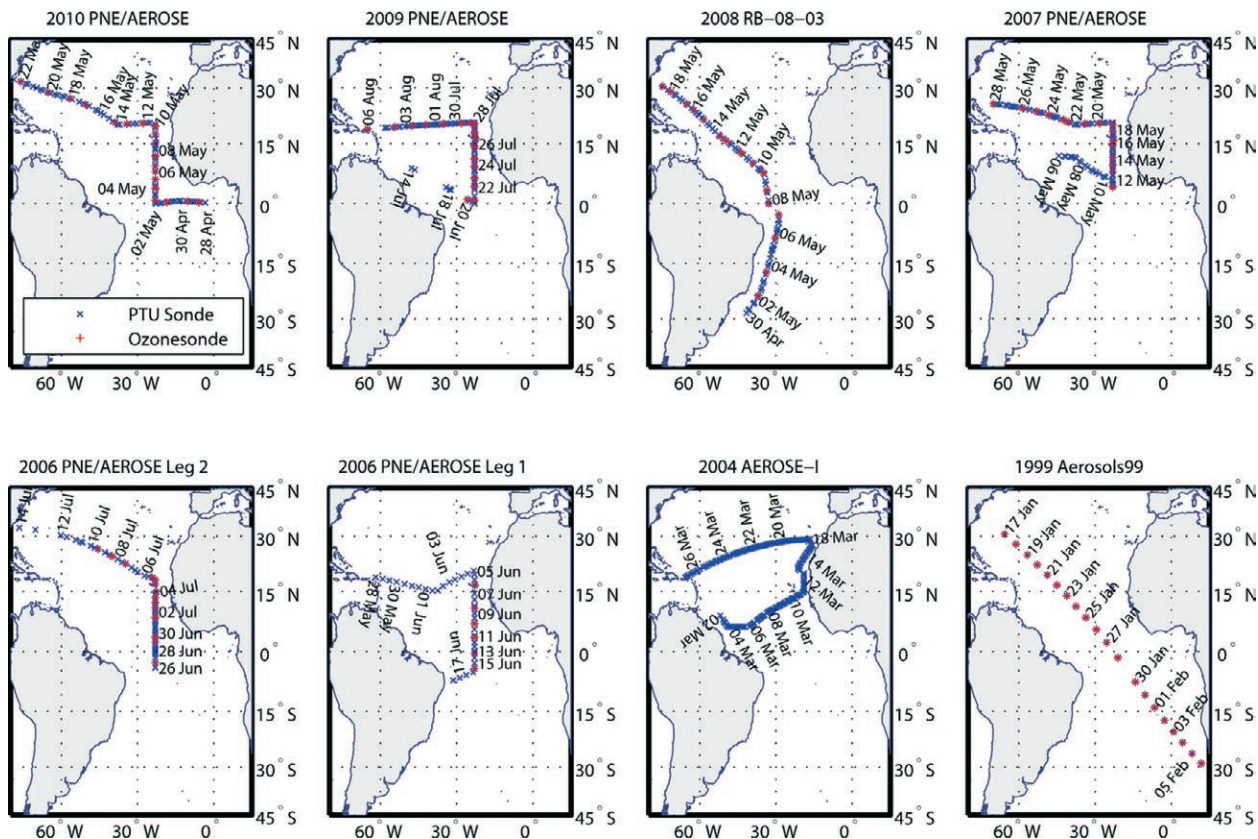


FIG. 2. Locations and dates of Vaisala PTU rawinsondes (blue \times) and ozonesondes (red $+$) launched during the AEROSE 2004 and 2006–10 campaigns. Locations of PTU/O₃ launches from the Aerosols99 cruise are also shown in the lower right plot for comparison. Map projections are cylindrical equal area.

Vaisala ceilometers, active laser systems similar to lidars, provide observations of the cloud-base height as well as the vertical distribution aerosol optical properties in the lower troposphere [see, e.g., Markowicz et al. (2008) for discussion on the retrieval of aerosols from ceilometers]. Multiple independent broadband pyranometers and pyrgeometers measure downwelling solar (visible) and terrestrial (IR) radiation for radiative energy balance calculations at the surface. Finally, in situ chemical, bulk aerosol, and radiative surface data are acquired, as reported in Morris et al. (2006). Thermo Electron Corporation (TECO) measurements include an ozone photometer (ambient gas-phase O₃), a carbon monoxide IR spectrometer (ambient gas-phase CO), an NO_x Chemilumen analyzer (ambient NO and NO₂), and an SO₂ fluorometer (ambient gas-phase SO₂). Chemical, bulk, and aerobiological sampling is performed using quartz and Teflon filters. Condensation and laser particle counters measure surface aerosol number densities, and a Quartz Crystal Microbalance (QCM) cascade impactor measures surface aerosol mass densities.

Table 1 summarizes AEROSE atmospheric data particularly germane to satellite remote sensing (e.g., EDR product validation and radiative transfer studies). Focused analyses of these data are subjects planned for future papers.

SCIENCE HIGHLIGHTS. As already mentioned, the AEROSE study domain is a region of great meteorological interest. This section highlights some of the more salient phenomena captured by the PNE/AEROSE campaigns.

Saharan dust and sub-Saharan smoke. In the troposphere, seasonally persistent elevated levels of aerosols with residence times >1 day are found to occur in regions downwind of continental sources. The main sources of these tropospheric aerosols include aeolian mineral dust from deserts, smoke from biomass burning, and anthropogenic sources. Of these, dust from the Sahara Desert is the foremost source of global aerosols, which, along with the Arabian Desert, contributes a total mass of ≈2000 Tg per annum (e.g., Hobbs 2000). Smoke from biomass burning sites (e.g.,

TABLE I. AEROSE tropical Atlantic atmospheric data (2004, 2006–10).

Dates	Vaisala radiosondes ^a	EN-SCI ECC ozonesondes ^a	M- AERI ^b	Microtops ^{c,d}	Ceilometer ^{d,e}	LW/SW fluxes ^d
2004 Mar	156 (42,0)	0 (0,0)	24	21	0	25
2006 Jun–Jul	96 (69, 0)	20 (18, 0)	37	28	51	45
2007 May	96 (40, 43)	17 (7, 10)	24	18	30	27
2008 Apr–May	74 (33, 34)	16 (8, 8)	23	10	21	22
2009 Jul–Aug	81 (32, 33)	17 (8, 9)	0	17	25	26
2010 Apr–May	75 (36, 38)	19 (10, 9)	24	19	22	24
Totals	578 (252, 148)	89 (51, 36)	132	113	149	169

^aSuccessful launches; numbers in parentheses denote launches timed for *Aqua*/A-Train and MetOp overpasses, respectively. Vaisala RS92-SGP (GPS) radiosondes have been used for all campaigns except in 2004, which used RS80-H (GPS) and RS90 (non-GPS).

^bNumber of days with available quality-assured (QA) data; in 2009 the M-AERI suffered from unexpectedly high levels of instrument spectral random noise.

^cMultichannel $\tau_a(\lambda)$ for 2009–10 are at $\lambda = 340, 380, 440, 500, 675, 870, 1020, 1640$ nm; pre-2009 reprocessed multichannel data are at 339, 441, 674, 869 nm for years 2006–08 and 340, 380, 870, 1020 nm for 2004.

^dNumber of days measurements were taken.

^eAll campaigns used a Vaisala CL31 Laser Ceilometer with the exception of 2006, which used a CT25K Laser Ceilometer.

savanna grasslands in sub-Saharan Africa) contributes ≈ 200 –450 Tg per annum of biogenic aerosols of smaller, accumulation mode particles. The massive large-scale transport of dust and smoke from Africa across the Atlantic Ocean (the quantity of dust transport alone has been estimated at 100–400 Tg per annum; Prospero et al. 1981) are the primary subjects of AEROSE.

The magnitude, extent, and seasonal variation of trans-Atlantic African dust and smoke outflows are readily observed from space as in Fig. 3, which shows a 22-yr monthly AOD climatology (1981–2008 base period excluding the Mt. Pinatubo and El Chichon eruptions) for the tropical Atlantic Ocean and vicinity as derived from the NOAA Advanced Very High Resolution Radiometer (AVHRR) Pathfinder Atmospheres Extended (PATMOS-x) dataset (e.g., Jacobowitz et al. 2003; Zhao et al. 2008). These data show first and foremost that Saharan dust outflows are, in a mean sense, a persistent feature of the North Atlantic atmosphere, even during months of minimal activity. A seasonal cycle is apparent in that the main dust plume axis translates northward (southward) during the boreal summer (winter) months, remaining to the north of the intertropical convergence zone (ITCZ). These trans-Atlantic dust outflows, in terms of westward extent and maximum intensity, also gradually decrease from a maximum during Northern Hemisphere summer (June–July) to a minimum during the autumn (October–November) before increasing again in the spring, whereas dust outflows into the Gulf of Guinea

become prevalent during the months of December–March (as noted by Resch et al. 2008). African smoke outflows associated with sub-Saharan biomass burning gradually become apparent south of the ITCZ in the boreal spring before achieving a maximum in late summer (July–September), then gradually decrease again, minimizing in winter. Biomass burning in Africa also occurs north of the ITCZ during boreal winter months, resulting in some contribution to the Atlantic and Gulf of Guinea plumes during December–March (e.g., Resch et al. 2008), and burning over the Yucatan Peninsula becomes prominent during April–May. Finally, there is also an increase in aerosol outflows off the east coast of the United States during spring to early autumn months (March–September), presumably the result of increased anthropogenic smog from the urban corridor.

Figures 4 and 5 show daily mean AEROSE column AOD, $\tau_a(\lambda)$, and derived Angstrom exponents,

$$\alpha = -\frac{\ln[\tau_a(\lambda_1)/\tau_a(\lambda_2)]}{\ln(\lambda_1/\lambda_2)},$$

for selected meridional and zonal transects as measured from Microtops handheld sunphotometers and processed using the MAN methodology described by Smirnov et al. (2009). It is seen that the AEROSE campaigns have all encountered, to varying degrees, aerosol plumes due to dust and smoke outflows from Africa. This includes persistently elevated levels near the African coast, as in the 2006 and 2009–10

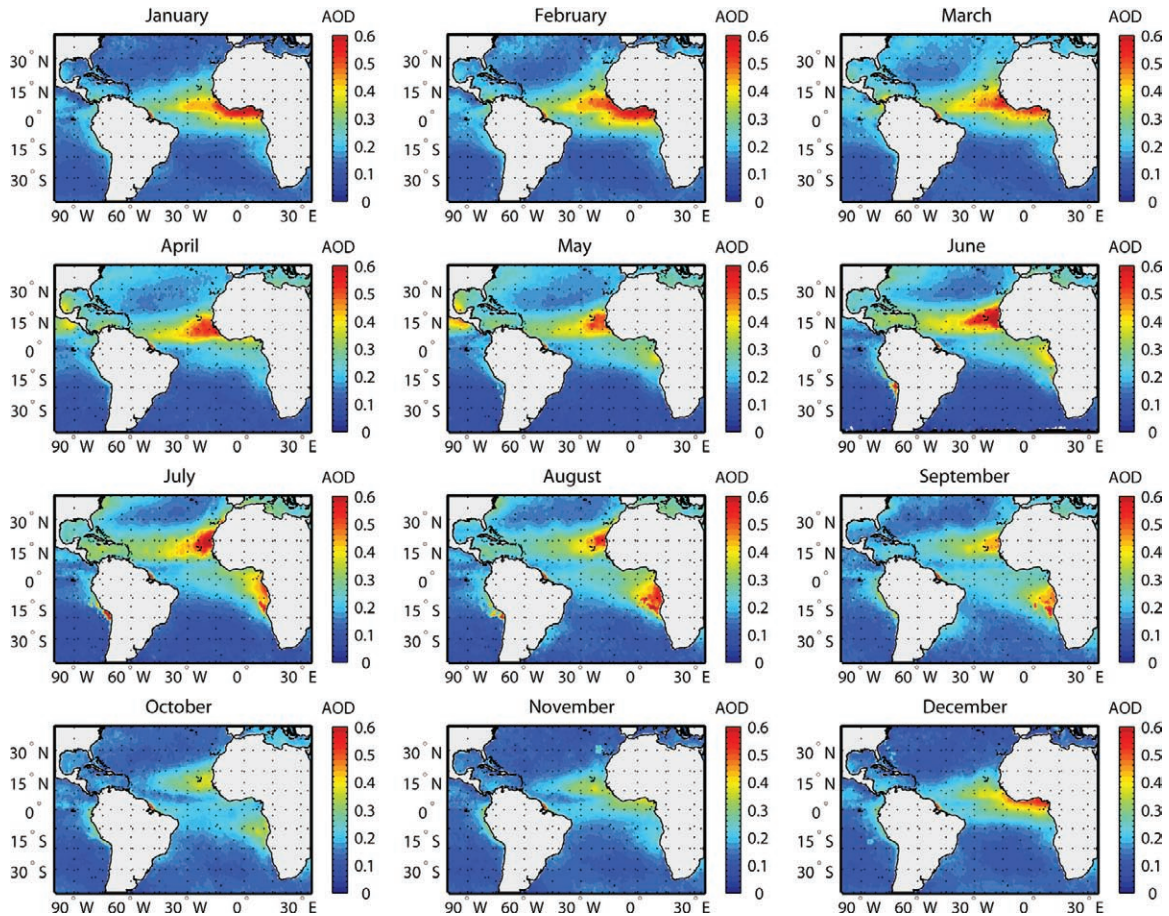


FIG. 3. AVHRR Pathfinder Atmospheres Extended (PATMOS-x) monthly climatological mean tropospheric aerosol optical depth (AOD) for a 1981–2008 base period, excluding years following volcanic eruptions, 1982–84 and 1991–93. The PATMOS-x AODs are derived from cloud-free AVHRR channel I ($\lambda = 0.63 \mu\text{m}$) normalized reflectances (cf. Jacobowitz et al. 2003; Zhao et al. 2008). Map projections are Mercator.

campaigns, as well as major dust pulses with AOD approaching or exceeding 1.0, as in the 2004 and 2007 campaigns. The multiyear measurements show patterns qualitatively consistent with the PATMOS-x climatology (Fig. 3) as well as similar earlier field measurements from the Aerosols99 cruise (cf. Voss et al. 2001), generally corroborating the aerosol regimes observed by Bates et al. (2001). The zonal plots (Fig. 4) show a tendency toward lower AOD and higher α (smaller, nondust particles) in the western North Atlantic basin, indicative of background marine aerosols (e.g., sea salt), or possibly industrial smoke and/or haze, as in 2010 (Fig. 4a). Encounters with dust plumes of varying degrees ($\tau_a \geq 0.3$, $\alpha \leq 0.3$) become more prevalent eastward of 45°W , with the exception of 2010 (Fig. 4a), when the ship was cruising westward at ≈ 13 kt under predominately westerly winds aloft. The meridional plots (Fig. 5), particularly those in the eastern Atlantic near the African coast, show persistently elevated aerosol levels associated

with Saharan dust ($\tau_a \geq 0.3$, $\alpha \geq 0.3$, typically north of the ITCZ), smoke from biomass burning ($\tau_a \geq 0.3$, $\alpha \geq 0.5$, typically south of the ITCZ), or some combination of both. The 2008 interhemispheric transit (Fig. 5a) shows a small local peak in AOD at 10°N , $\tau_a \approx 0.3$ and $\alpha \approx 0.15$, these values being similar to that observed during Aerosols99 (cf. Voss et al. 2001), the result of remnant dust over the mid-Atlantic.

The dust pulse encountered during 2004 AEROSE-I (Fig. 4f) was intense for the time of year (early March), and yet one of greater magnitude was encountered in May 2007 just prior to and during the northbound 23°W transect of PNE/AEROSE-III (Fig. 5c). Figure 6 shows a 13 May 2007 Meteosat SEVIRI color-composite red–green–blue (RGB) image with the location and time of a concurrent radiosonde launch overlaid. It is seen that this sounding (skew T plot given below in Fig. 8) was obtained within a very dusty, yet virtually cloud-free, air column well to the north of the ITCZ. For comparison, Fig. 7 shows a nearly coincident

digital color photograph of the dust outflow from the vantage point of the *Ronald H. Brown* while holding station along 23°W. The very low visibility near the horizon indicates the settling of dust into the surface layer of the marine boundary layer (MBL), as also verified by concurrent ceilometer and particle measuring system (PMS) (data not shown here). Consistent with Fig. 6, there are very few if any detectable low to midlevel clouds within the camera field of view (FOV). We will return to this dust event in the overview and analysis of the entire complement of PNE/AEROSE RAOBs presented in the next subsection.

The Saharan air layer and the distribution of tropospheric water vapor. The general distribution of tropical tropospheric RH is a topic of substantial concern,

especially as it pertains to potential feedbacks in response to climate change (e.g., see Pierrehumbert and Roca 1998; Sherwood et al. 2006; Pierrehumbert et al. 2007; Dessler and Sherwood 2009) and its impact on tropical cyclogenesis and convection. Of particular interest over the tropical North Atlantic is the SAL, a stable layer of dry, warm air that often accompanies Saharan dust aerosols and advects across the Atlantic basin, as first noted by Carlson and Prospero (1972). These conditions are believed to suppress hurricane activity over the Atlantic (e.g., Karyampudi and Pierce 2002; Dunion and Velden 2004; Wong and Dessler 2005; Evan et al. 2006; Wu 2007; Sun et al. 2008) and may also be self-sustaining as a result of reduced radiative cooling in the layer (e.g., Mapes and Zuidema 1996; Wong et al. 2009). While there have

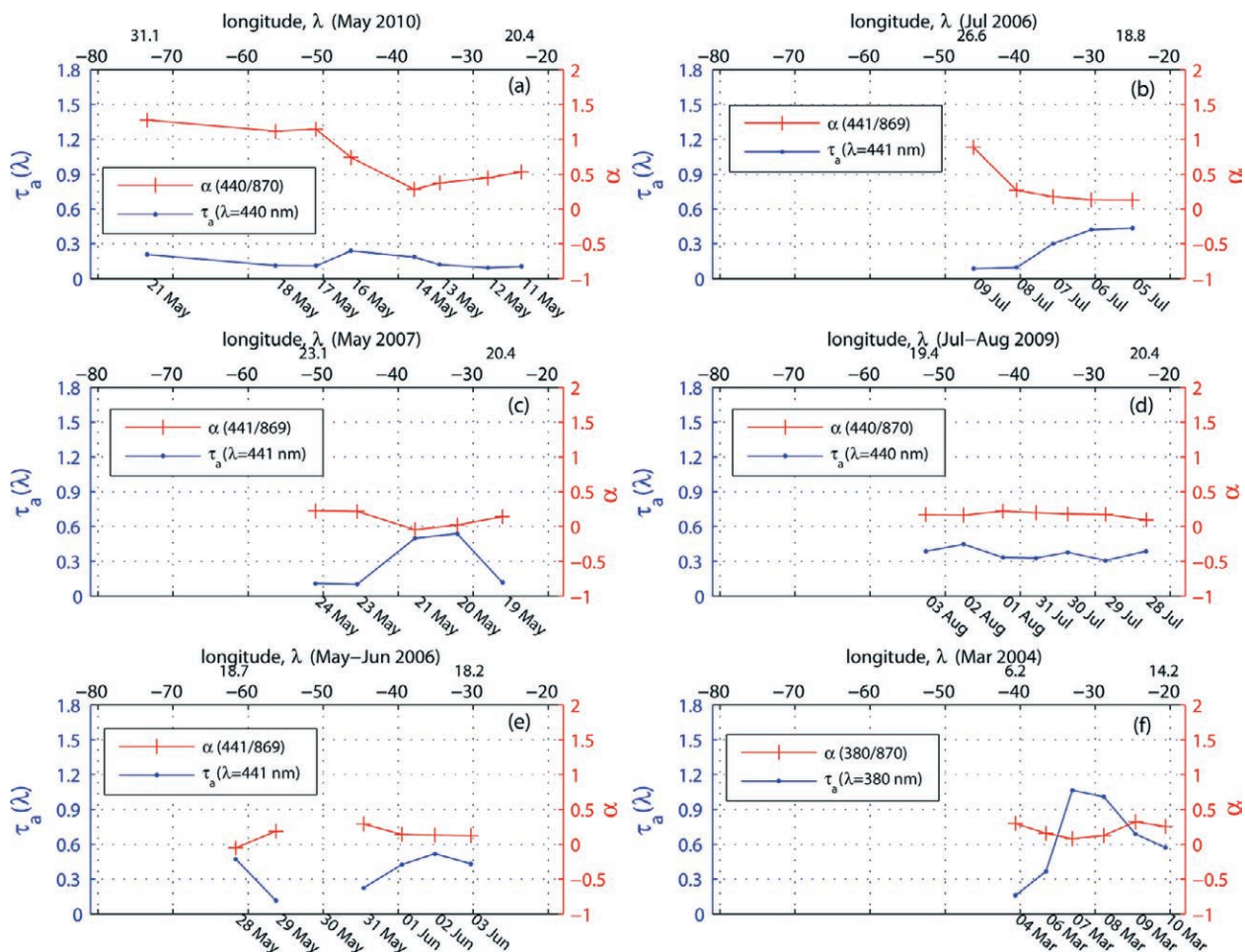


FIG. 4. Microtops sunphotometer daily mean AOD (τ_a , blue) and derived Angstrom exponents (α , red) for selected zonal AEROSE transects plotted on a common longitude scale. Small numbers above the main x axis labeling denote the limits of the orthogonal axis (i.e., latitude). Raw AOD values have been processed according to the MAN standard methodology (Smirnov et al. 2009). The plots are roughly “sorted” from left to right and top to bottom as north to south zonal sections: (a) May 2010 [20.45°N, 31.09°N], (b) Jul 2006 [18.79°N, 26.57°N], (c) May 2007 [20.40°N, 23.06°N], (d) Jul–Aug 2009 [19.39°N, 20.44°N], (e) May–Jun 2006 [18.23°N, 18.73°N], (f) Mar 2004 [6.16°N, 14.22°N].

been a number of recent papers that have described the SAL based on soundings over the region (e.g., Dunion and Marron 2008, hereafter DM08; Zipser et al. 2009), high-resolution in situ space–time cross sections of the SAL were obtained for the first time over the eastern Atlantic basin from 3-hourly (8 per day) RAOBs launched during the 2004 AEROSE-I campaign [as reported in Nalli et al. (2005)]. Hyper/ultraspectral sounding systems in LEO configuration (e.g., IASI/AIRS/CrIMSS), as well as geosynchronous imagers (e.g., ABI, SEVIRI), are valuable tools whereby the SAL and the distribution of tropospheric water vapor can be routinely observed in this manner (e.g., Pierrehumbert and Roca 1998; Dunion and Velden 2004; Zhang and Pennington 2004; Nalli et al. 2006; Sherwood et al. 2006), thus furthering the need for satellite validation correlative data in this region (e.g., Nalli et al. 2006; Wu 2009).

Figure 8 shows skew T - $\log p$ diagrams of two sample soundings obtained from the PNE/AEROSE-III and -V campaigns alongside the recently published DM08 July–October mean tropical Caribbean sounding for SAL environments during hurricane season (DM08) for reference. The DM08 mean SAL sounding (far right) is the result of soundings obtained from stations in Miami, Grand Cayman, San Juan, and Guadeloupe, spanning a region similar to that considered by Jordan (1958), during SAL conditions as ascertained from GOES satellite. The leftmost skew T plot shows an AEROSE Caribbean RAOB launched at 0342 UTC 6 August 2009. This sounding was the final and westernmost sonde launch of the AEROSE-V campaign⁶ (18.75°N, 65.12°W), only \approx 105 km offshore

⁶ Being launched immediately upon clearing the Barbuda exclusive economic zone (EEZ).

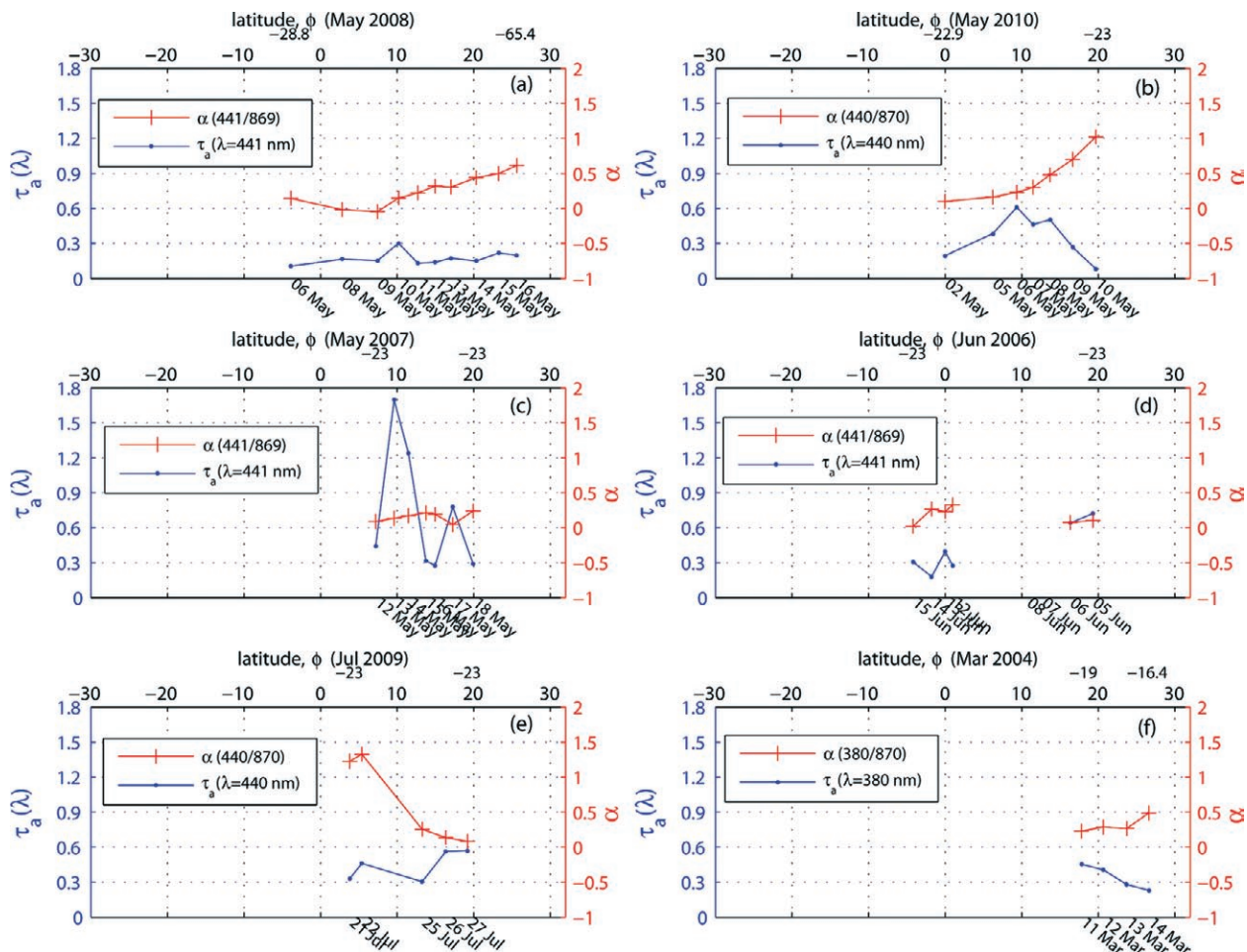


FIG. 5. As in Fig. 4, but for meridional AEROSE transects plotted on a common latitude scale. Small numbers above the main x axis labeling denote the limits of the orthogonal axis (i.e., longitude). The plots are roughly sorted from left to right and top to bottom as first west to east meridional sections and then time of the year: (a) May 2008 [28.83°W, 65.41°W], (b) May 2010 [22.93°W, 23.03°W], (c) May 2007 [23.00°W, 23.00°W], (d) Jun 2006 [23.00°W, 23.00°W], (e) Jul 2009 [23.00°W, 23.01°W], (f) Mar 2004 [19.00°W, 16.39°W].

SEVIRI RGB Composite - 13 May 07 13:12

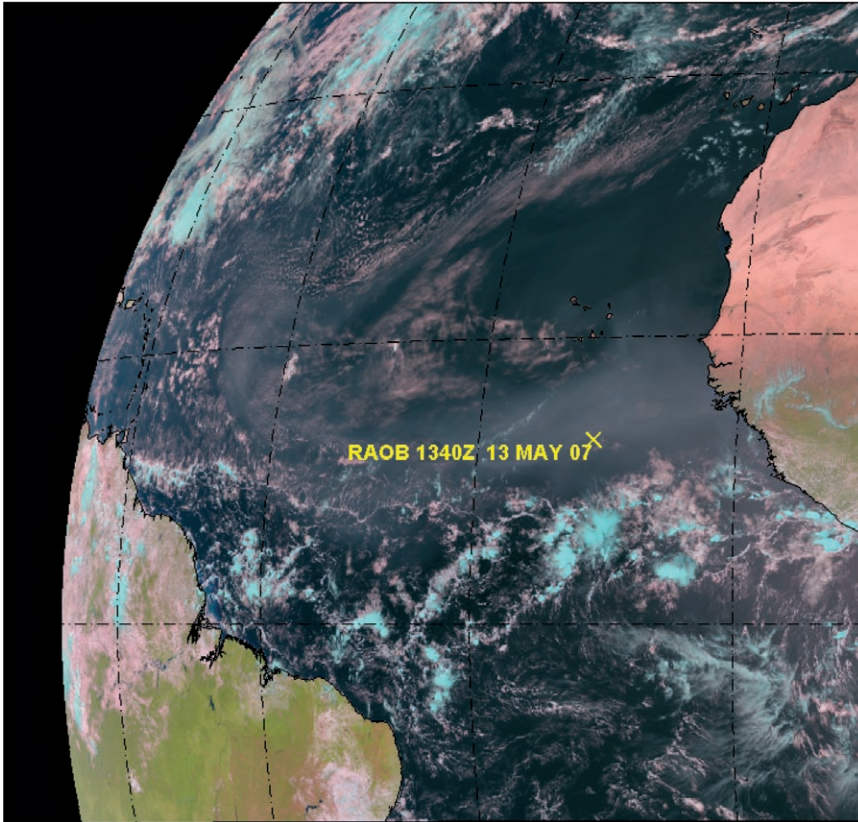
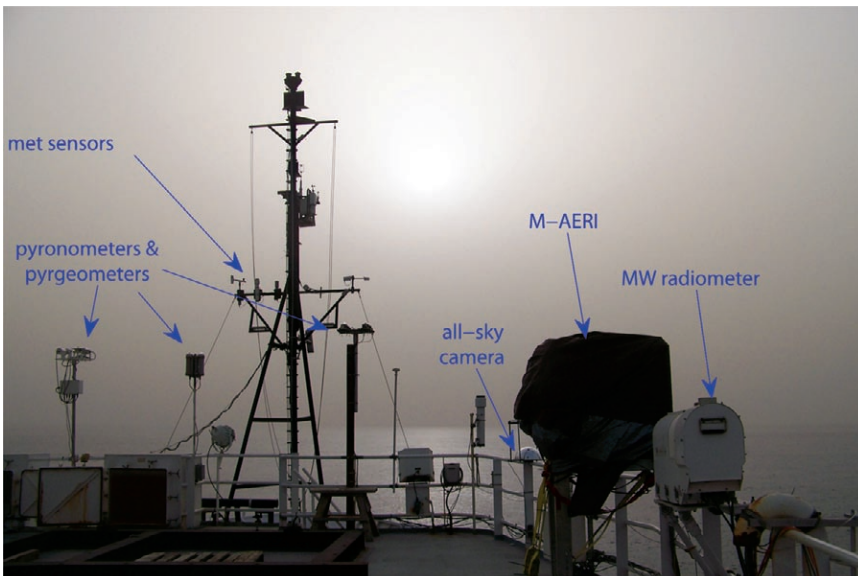


FIG. 6. SEVIRI RGB color-composite (using channels 1.6, 0.8, and 0.6 μm for red, green, and blue, respectively) 2-km imagery for the AEROSE domain, 1312 UTC 13 May 2007. The location of a coincident sonde launch (9.501°N, 22.998°W; 1340 UTC) is shown in yellow. Map projection is vertical perspective azimuthal. NESDIS/STAR has archived hourly 2-km SEVIRI multichannel data for all the AEROSE campaigns to create a marine-based GOES-R proxy dataset for pre-launch validation of the GOES-R ABI (Nalli et al. 2008b).



from San Juan, Puerto Rico (18.45°N, 66.07°W). It is interesting to see striking similarity between this RAOB and the DM08 mean SAL sounding in terms of the location and strength of tropospheric dryness, the temperature profile, and prevailing easterly winds throughout the lower troposphere, although the finescale variability, including moist filaments (cf. Pierrehumbert 1998; Pierrehumbert and Roca 1998), apparent in the AEROSE sounding has been lost in the smoothed mean sounding. It is reasonable that the driest layers in the AEROSE sounding above 600 hPa are associated, at least in part, with large-scale advection and subsidence drying in the Hadley circulation, this being consistent with the “advection–condensation” model formulated in a number of earlier papers such as Pierrehumbert and Roca (1998), Sherwood et al. (2006), and Pierrehumbert et al. (2007).

The similarity between the two soundings, however,

FIG. 7. Unenhanced digital color photograph of the forward 02 level of the *Ronald H. Brown*, taken while holding station along 23°W longitude during PNE/AEROSE-III, on the afternoon of 13 May 2007, during the major Saharan dust outflow pulse shown in Fig. 6. Some AEROSE instrumentation visible in the foreground, from left: broadband flux radiometers (i.e., pyrometers and pyrgeometers), all-sky camera, M-AERI, and microwave (MW) radiometer.

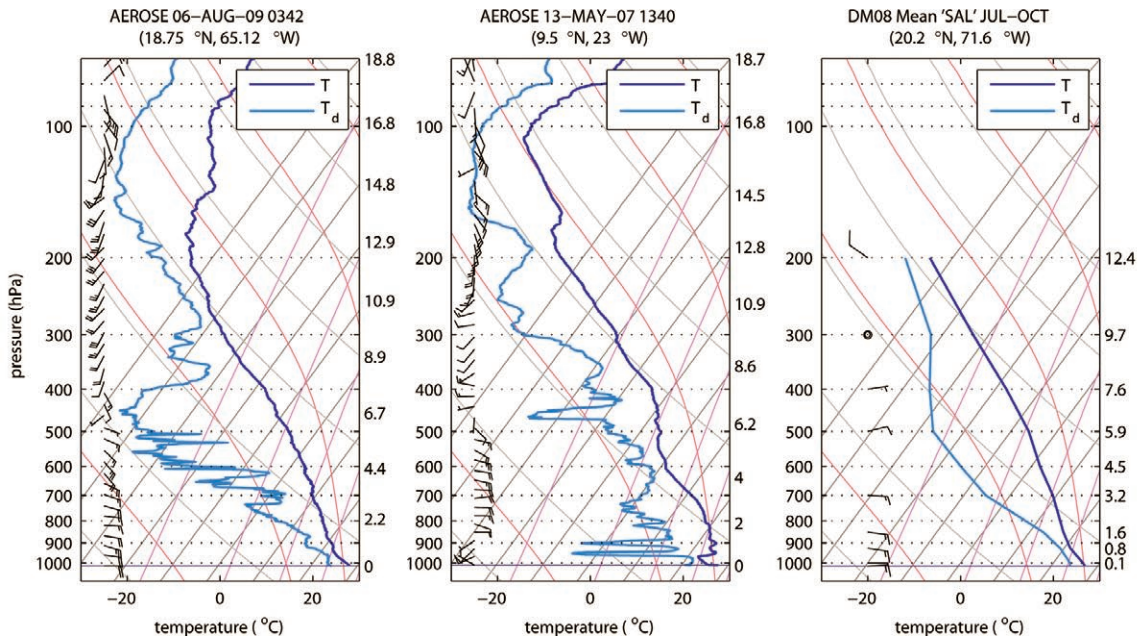


FIG. 8. Skew- $T \log p$ diagrams of tropical Atlantic/Caribbean soundings: (left) AEROSE-V (0342 UTC 6 Aug 2009) sounding from western Atlantic (Caribbean Sea) just northeast of Puerto Rico (18.75°N , 65.12°W); (center) AEROSE-III (1340 UTC 13 May 2007) sounding from the eastern Atlantic (9.5°N , 23.00°W) during major dust outflow (cf. Figs. 6 and 7); and (right) Jul–Oct 2002 mean sounding (Caribbean Sea) for SAL conditions during the Atlantic hurricane season (DM08). The right-hand y axes show geopotential heights (in km) for reference. Conventional wind barbs designate metric wind speeds rounded to the nearest 2.5 and 5.0 m s^{-1} for half and full feathers, respectively.

disappears altogether when we compare the RAOB from the eastern Atlantic (Fig. 8, middle), a sonde launched along the 23°W south–north transect in the midst of intense dust outflow during the AEROSE-III campaign, at 1340 UTC 13 May 2007 (cf. Figs. 6 and 7). In this sounding it is apparent that there are multiple dry layers, notably starting in the upper troposphere at 200–300 hPa, followed by a strong one at ≈ 450 hPa, and a warm, moderately dry layer from 700 hPa down to the MBL inversion, with two embedded extremely dry filaments at 900 and 950 hPa. The multiple dry layers in this sounding are, generally speaking, all associated with well-defined inversions at their base [these characteristics also being observed by Mapes and Zuidema (1996)], with temperatures in the low-level warm dry layer between 950 and 700 hPa substantially warmer than either the Caribbean sounding (left) or the DM08 mean SAL sounding (right). It will be seen below in cross-sectional analyses that this RAOB is actually within the heaviest dust outflow to the north of the ITCZ and at the southern boundary of a very pronounced SAL extending well north of this location and reaching altitudes of 4 km. This case (as with the zonal cross sections below) also suggests that another tropical mean sounding, valid for the eastern Atlantic

basin, may in fact be desirable (as already hinted at by DM08); the full complement of AEROSE soundings may serve ideally for this purpose.

TRANS-ATLANTIC RAOB CROSS SECTIONS: RH, VPTRL, AND WIND. As mentioned above, the RAOB launch frequency of each PNE/AEROSE campaign enables space–time cross-sectional analyses. As in Nalli et al. (2005), cross sections are here generated by first preprocessing the sonde PTU data via least squares linear polynomial smoothing followed by linear interpolation to a common height coordinate. Figures 9 and 10 show the zonal cross sections (longitude scales and transect subplot ordering identical to Fig. 4) of tropospheric moisture (RH) and virtual potential temperature lapse rate (VPTRL), respectively. VPTRL is a direct indicator of local static stability (e.g., Stull 1991; Pan et al. 2009) defined as $\delta\theta_v(z)/\delta z$, where $\theta_v(z)$ is the virtual potential temperature sounding and z is taken to be the geopotential height. Likewise, Figs. 11 and 12 show the meridional cross sections (latitude scales and transect subplot ordering identical to Fig. 5) of RH and VPTRL, respectively.

While case studies of the orthogonal cross sections for specific campaigns can provide some insight into a given atmosphere’s 4D synoptic structure at

mesoscale resolution, we attempt here only to highlight key features and patterns found in the ensemble zonal and meridional sections. The latitude zone of the ITCZ axis for the 2006–10 campaigns can be seen clearly in Figs. 11a–e, with a deep column of moist air extending from the surface up to the upper troposphere, and in some cases what is presumably a divergence of moisture plumes northward and southward at the top (Figs. 11b,d,e). Beneath these moisture plumes flanking the ITCZ column are relatively deep layers of very dry air in the mid to upper troposphere (consistent with Mapes and Zuidema 1996; Pierrehumbert 1998; Pierrehumbert and Roca

1998; Sherwood et al. 2006), with inversions present at their bases (Fig. 12), probably resulting from net radiative heating as well as subsidence (as shown by Mapes and Zuidema 1996) and usually starting around 5 km (Figs. 12b–f).

Of particular interest to AEROSÉ is the SAL, which is seen to be a common feature in these cross sections as low-level “filaments” or “tongues” (i.e., shallow layers) of very dry air with very strong inversions just above the MBL on the north side of the ITCZ. Mapes and Zuidema (1996) asserted that such dry tongues within the tropical Pacific warm-pool atmosphere result mostly from advection, and

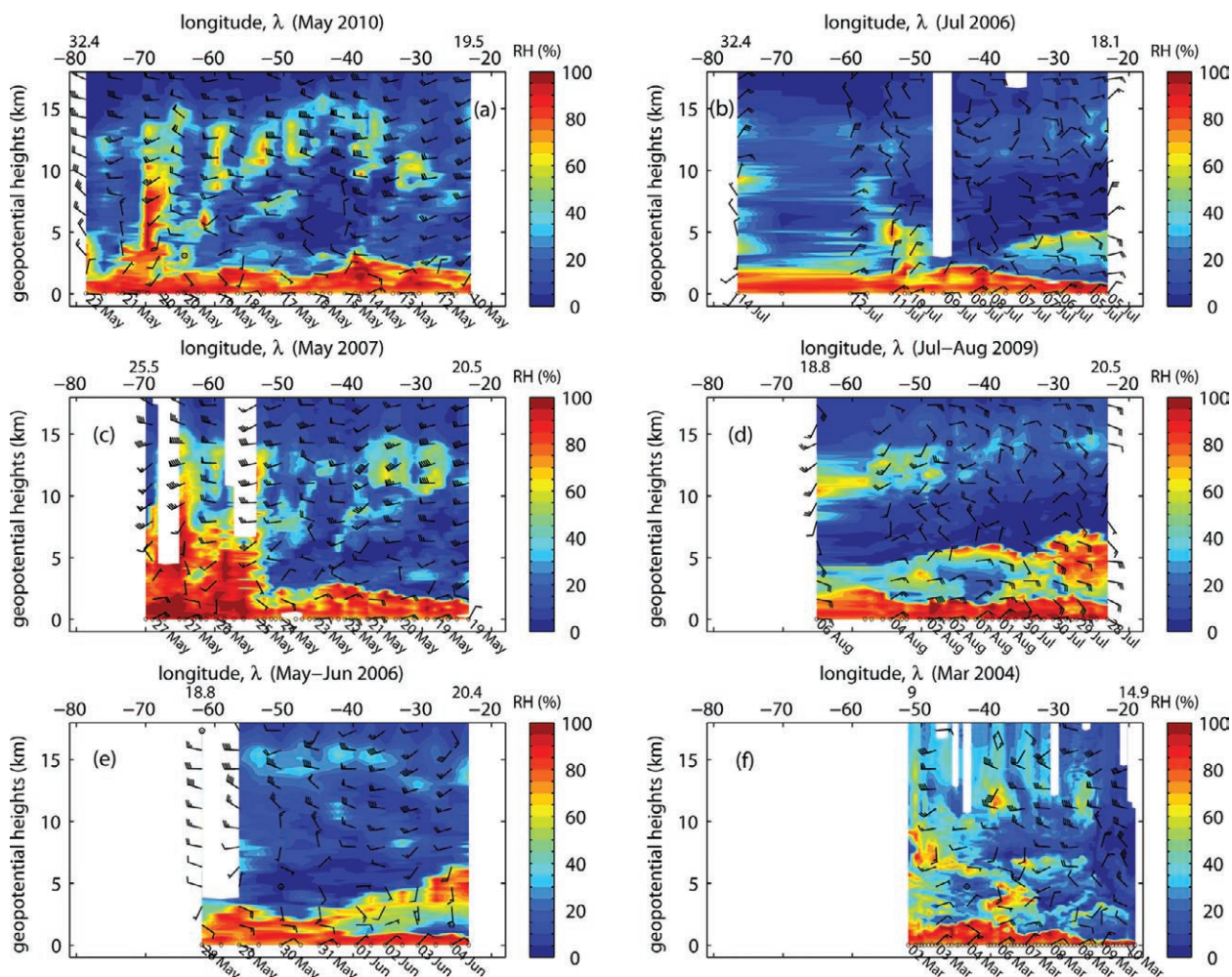


FIG. 9. Zonal cross-sectional contour analyses of Vaisala radiosonde RH measurements (%), expressed as a function of longitude and geopotential heights, z_g (km), obtained during the AEROSÉ campaigns. Small numbers above the main x-axis labeling denote the limits of the orthogonal axis (i.e., latitude). Horizontal-component wind vector measurements are overlaid (for clarity, only a subsample of wind vectors is shown); speeds are expressed in SI units using half, full, and pennant feathers for increments of 2.5, 5.0, and 25 m s^{-1} , respectively. Sonde launch locations are shown by small circles at the surface; dates are shown for the wind vector subsamples. Longitude scales and transect subplot ordering are as in Fig. 4: (a) May 2010 [19.50°N, 32.44°N], (b) Jul 2006 [18.08°N, 32.42°N], (c) May 2007 [20.49°N, 25.48°N], (d) Jul–Aug 2009 [18.75°N, 20.46°N], (e) May–Jun 2006 [18.76°N, 20.41°N], (f) Mar 2004 [9.01°N, 14.94°N].

indeed it is our observation that the SAL appears to be a persistent and extreme case of this “dry-tongue” phenomenon in the North Atlantic. The depth of the SAL appears to vary from extremely shallow ($\delta z < 1$ km) but horizontally extensive ($\delta\phi \geq 5^\circ$) layers, as in May 2010 (Fig. 11b, below 2 km at 9° – 16° N), to deeper layers $\delta z > 2$ km as in Figs. 11a and 11c–f. Easterly winds are often, but not always, prevalent within the low-level dry layers. The transects near the African coast show a stronger SAL (as measured by the VPTLR in Fig. 12) with the inversion base at very low altitudes, the lowest being the May 2007 and March 2004 cases (Figs. 12c and 12f, respectively). The March 2004 transect was closest to the African coast, and indeed the temperature inversion (MBL inversion strengthened by the SAL) begins immediately at the surface with the sharp discontinuity between moist MBL and dry SAL at ≈ 0.2 km (Fig. 12f). The May 2007 transect was highlighted above in the skew- T plot of the 1340 UTC 13 May 2007 sounding launched

at 9.50° N, 23.00° W (Fig. 8, middle), and images of the concurrent dust plume from Meteosat (Fig. 6) and the *Ronald H. Brown* (Fig. 7). We may now see this isolated sounding in its fuller context as located north of the ITCZ with the low-level dry filaments found at the southern lower edge of a prominent SAL extending from ≈ 0.35 to 4.0 km and 10° N to beyond 20° N (Fig. 11c), as well as a deep region of large-scale subsidence drying in the mid to upper levels (Fig. 11c), these both being associated with two strong inversions, one at the MBL interface and the other in the midtroposphere around 5 km (Fig. 12c), features similar to those described by Mapes and Zuidema (1996). However, as mentioned above, the heaviest (daytime) dust outflow was observed at the ship location around 13 May 2007 at $\approx 10^\circ$ N (e.g., Figs. 6, 7, and 5c), thereby presenting a case where the driest air column does not necessarily coincide with the heaviest dust column (as also observed by Zhang and Pennington 2004).

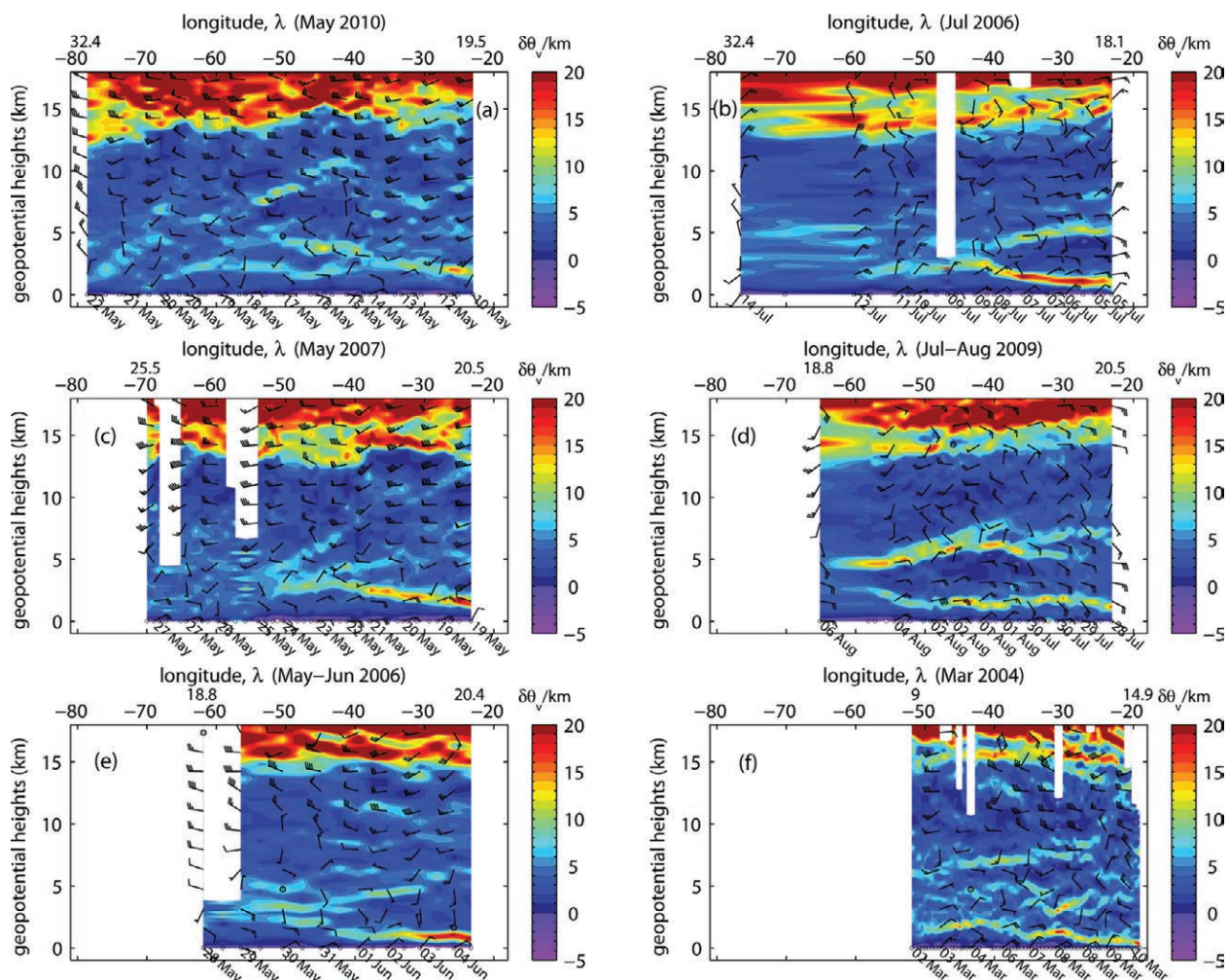


FIG. 10. As in Fig. 9, but for virtual potential temperature lapse rate (VPTLR), $\delta\theta_v/\delta z$.

The selected zonal cross sections shown in Figs. 9 and 10 were all obtained to the north of the ITCZ. With the exception of isolated areas of obvious convection extending from the surface upward and moist plumes aloft, these cross sections show dry air at mid to upper levels (generally $z > 3$ km), with well-defined inversions at their bases, spanning much of the tropical to subtropical North Atlantic basin. These are not necessarily Saharan in origin but may also be the result of large-scale subsidence associated with Hadley circulation (cf. Sherwood et al. 2006) or large-scale advection from elsewhere in the subtropics (cf. Mapes and Zuidema 1996). As above, the SAL is thus believed to be confined mostly to levels sandwiched between the MBL and ≈ 5 km. If we turn to the VPTLR cross sections (Fig. 10) and assume strong VPTLR above the MBL results from advection of Saharan (dry,

warm) air at low levels that is radiatively maintained or strengthened [as reported by Mapes and Zuidema (1996); Wong et al. 2009], then we may infer that SALs were present, to varying degrees and extents, in all the transects (with the exception of the Gulf of Guinea, not shown), some extending as far as 40°W (e.g., Figs. 10b–d).

TRANS-ATLANTIC SATELLITE IR SOUNDER CROSS SECTIONS: RH. As mentioned elsewhere in this paper, the AEROSÉ soundings are timed to coincide with overpasses of the *Aqua*/A-Train and MetOp LEO satellites, providing correlative data over open ocean useful for validation of passive IR sounding systems (viz., AIRS, IASI, CrIMSS, GOES-R ABI). Given the mesoscale synoptic observing missions of these satellite observing systems, we here perform

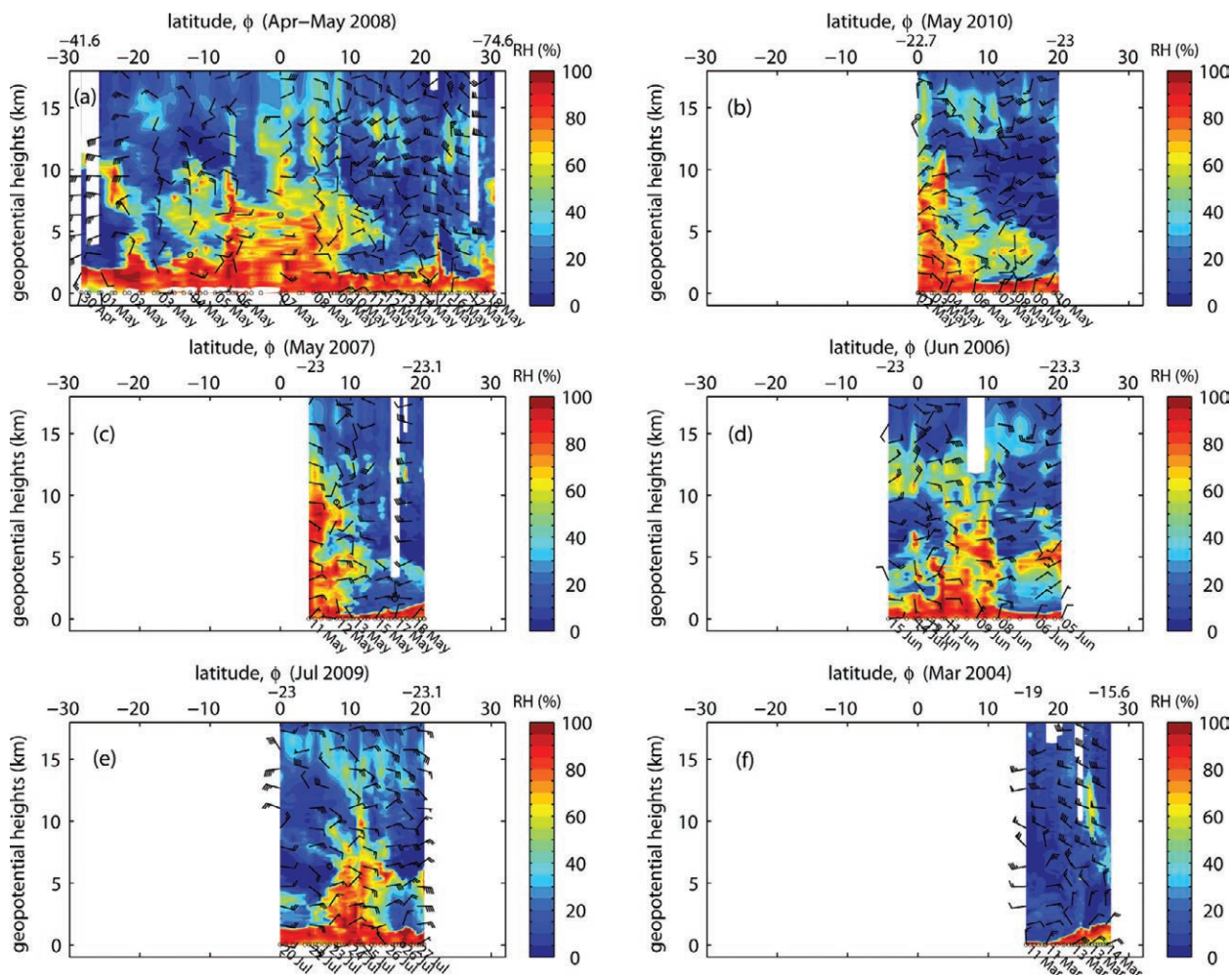


FIG. 11. As in Fig. 9, but showing meridional cross sections, with small numbers above the main x-axis labeling denoting the limits of the orthogonal axis (i.e., longitude). Latitude scales and transect subplot ordering are as in Fig. 5: (a) Apr–May 2008 [41.56°W , 74.63°W], (b) May 2010 [22.66°W , 23.00°W], (c) May 2007 [22.98°W , 23.07°W] (d) Jun 2006 [23.00°W , 23.29°W], (e) Jul 2009 [23.00°W , 23.11°W] (f) Mar 2004 [15.63°W , 19.00°W].

a qualitative validation demonstration using IASI data whereby we attempt to reproduce the AEROSE RAOB cross sections described in the previous section based on retrieval matchups. In this work, NOAA-unique IASI profile retrieval products are used from the NESDIS/STAR IASI Operational Product Processing System (e.g., King et al. 2008). Figure 13 shows zonal and meridional cross-sectional analyses of IASI-derived tropospheric RH (calculated from the retrieved temperature and water vapor mixing ratios) based on the nearest IASI field of regard (FOR) passing QA collocated with sonde launches (within 200 km) for a selection of the AEROSE transects shown in Figs. 9a, 9d, 11b, and 11c. Generally speaking, the NOAA IASI retrieved cross sections can be seen to capture much of the large-scale phenomena described above, including the ITCZ and moisture plume advection aloft, the deep layers of subsidence drying, and the MBL height. Under certain circumstances the NOAA IASI

retrievals resolve the SAL, as in July–August 2009 (Fig. 13c vs Fig. 9d; 38°–47°W from 2 to 4 km) or May 2007 (Fig. 13d vs Fig. 11c; 10°–20°W from 1.5 to 4 km). However, for the May 2010 case (Fig. 13b), the NOAA IASI retrievals miss the very shallow SAL dry filament seen in Fig. 11b, which is expected given the known theoretical resolving limits of passive IR sounders (e.g., Huang et al. 1992; Maddy and Barnet 2008). In making these comparisons it must be borne in mind that the IASI retrievals are at a much reduced horizontal spacing due to twice as many RAOBs being launched (RAOB launches being ≈ 4 per day to include AIRS overpasses). The NOAA IASI retrievals tend to have higher relative humidities in the upper troposphere, which may be due to a combination of factors; correlative data from campaigns such as AEROSE will be used for helping to improve the retrieval products. The impact of dust on the retrievals has not been isolated in these plots, but it will be the subject of ongoing research.

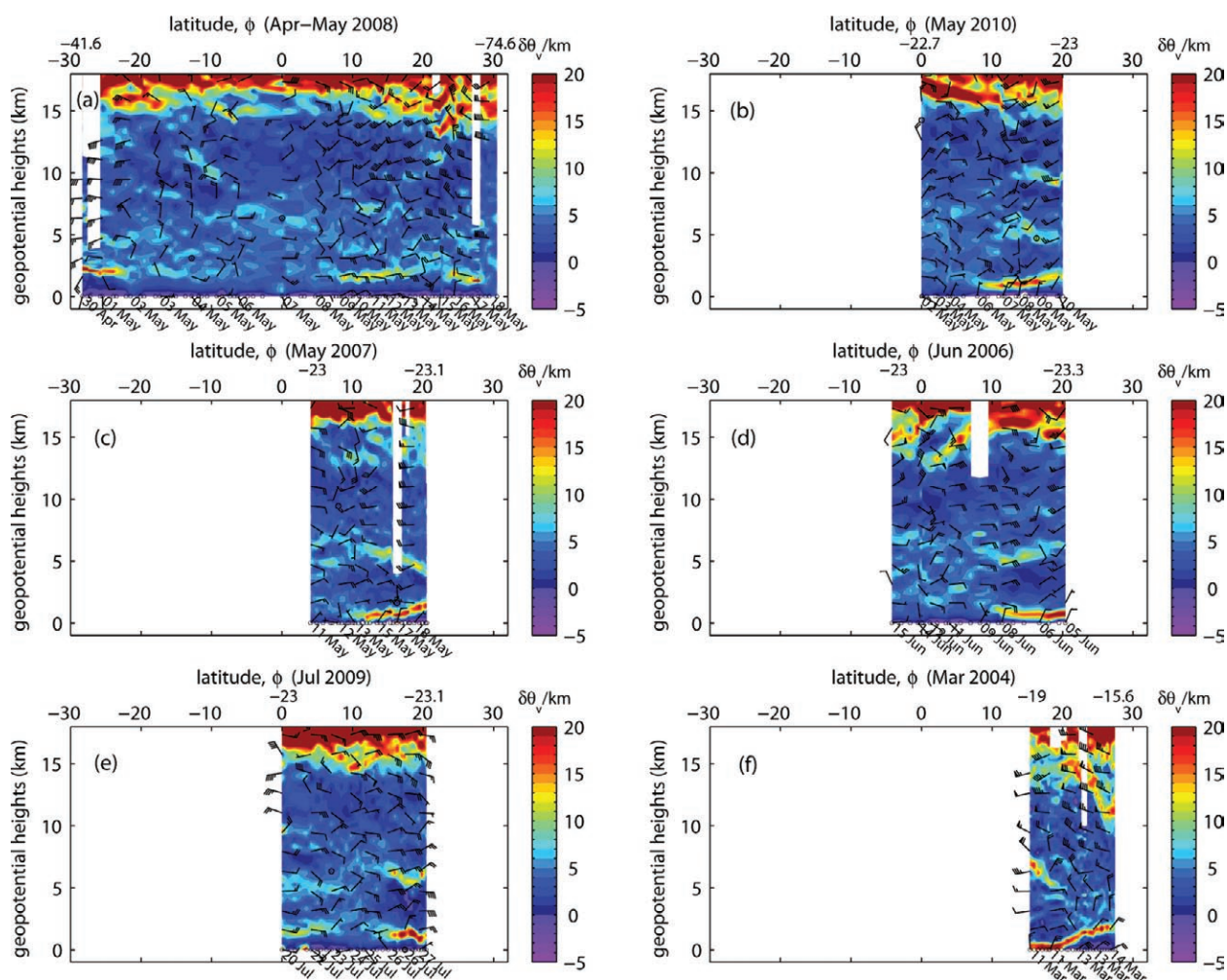


FIG. 12. As in Fig. 11, but for VPTLR, $\delta\theta_v/\delta z$.

Tropospheric ozone dynamics. The “tropical Atlantic ozone paradox” and “zonal wave one” are related tropospheric phenomena that have been the subject of considerable recent research (e.g., Jonquière et al. 1998; Thompson et al. 2000, 2003; Jenkins and Ryu 2004; Sauvage et al. 2006; Ziemke et al. 2006; Jourdain et al. 2007; Jenkins et al. 2008). Roughly speaking, the term “paradox” refers to an unexpected seasonal periodic behavior in free tropospheric O_3 over the tropical North and South Atlantic, assuming tropospheric ozone formation from ozone precursors arising from biomass burning.

Whereas the full nature of this phenomenon does not appear to be completely understood, it is the observation of higher tropospheric O_3 in the SH during the NH burning season over the tropical Atlantic that has been considered “paradoxical” (cf. Thompson

et al. 2003; Sauvage et al. 2006; Jourdain et al. 2007). In addition to the apparent paradox, the observed seasonal variation in the tropical–zonal distribution of tropospheric ozone, at least in the SH, has been described as a zonal wave one (e.g., Thompson et al. 2000, 2003; Ziemke et al. 2006), with the ridge axis occurring over the mid–South Atlantic, maximum amplitude occurring in September–November (SON), and a trough (presumably) located over the Pacific Ocean (cf. Sauvage et al. 2006; Ziemke et al. 2006; Jourdain et al. 2007). Based on satellite and limited in situ data records, the tropical O_3 wave one and associated Atlantic paradox have been described as “a common Atlantic feature” and “a predominantly SH phenomenon” (Sauvage et al. 2006), even though biomass “burning in the northern and southern Africa tropical belts is very similar” (Jonquière et al. 1998).

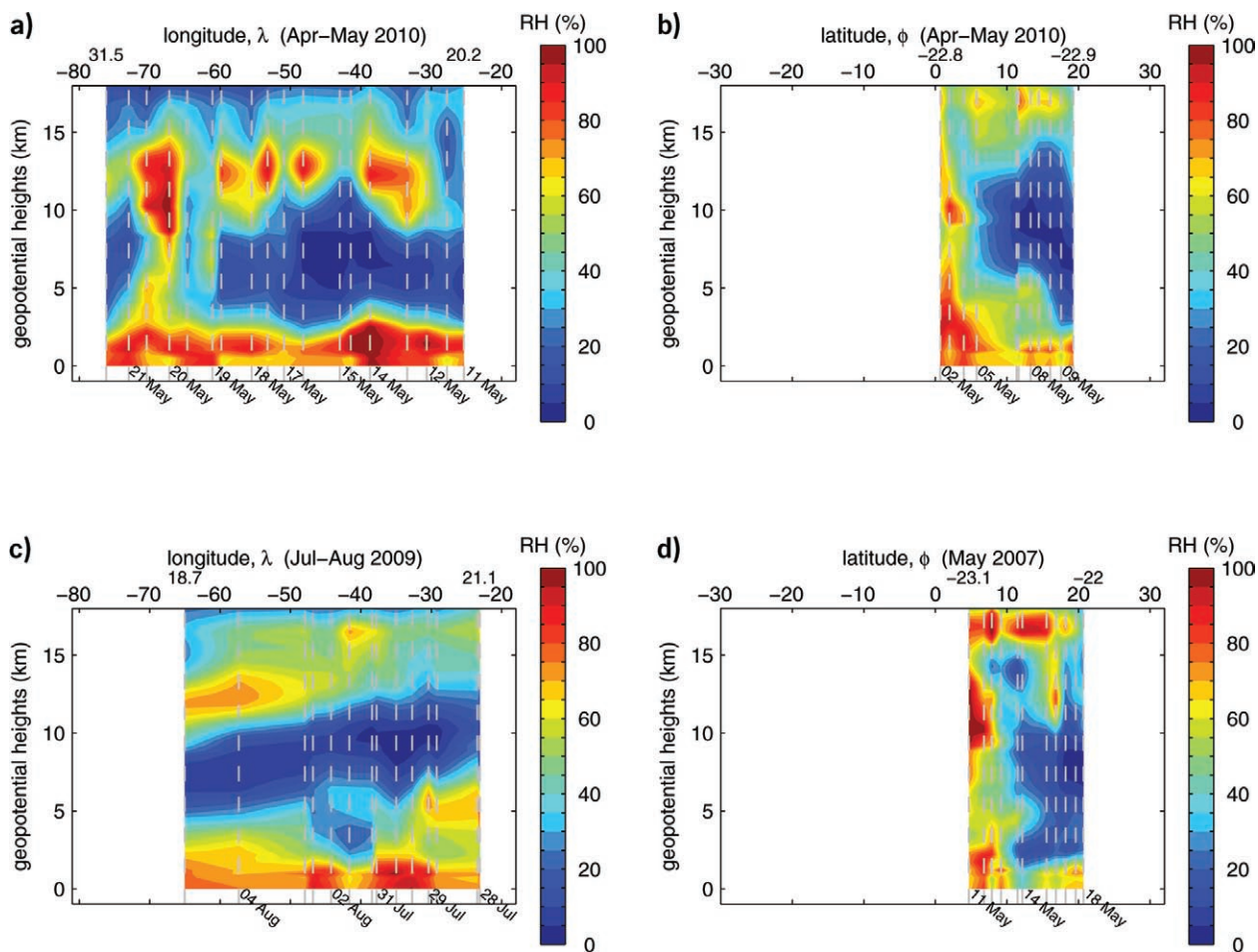


FIG. 13. As in Figs. 9 and 11, but showing contour analyses of IASI RH (derived from NOAA unique temperature and mixing ratio retrieval products obtained from the NESDIS/STAR IASI Operational Processing System) matched up with AROSE RAOB launches (nearest FOR passing QA and within 200 km) for selected cross sections (dating from 2007 on, after IASI went operational). Left and right columns show zonal and meridional cross sections, respectively: (a) Apr–May 2010 zonal, (b) Apr–May 2010 meridional, (c) Jul–Aug 2009 zonal, (d) May 2007 meridional. Retrieval locations are shown by grey vertical dashed lines.

During the Aerosols99 interhemispheric cruise, Thompson et al. (2000) noted that the highest SH tropospheric O_3 is observed from both in situ ozonesonde and satellites during boreal autumn, 2–3 months after peak regional biomass burning. Jenkins and Ryu (2004) extended the “Atlantic paradox” conceptual model to the NH by observing that seasonally elevated total column ozone (TCO) values in the NH (SH) occur during the periods of SH (NH) biomass burning. They attributed this behavior primarily to NO_x formation (an O_3 precursor) arising from seasonally consistent lightning patterns in central and western Africa, followed by advection via easterly winds. Monthly charts of satellite-derived TCO published by Ziemke et al. (2006) also show the transition of elevated zonal TCO from the SH to the NH during the seasonal march from September–November (SON) to June–August (JJA), and that this behavior is not isolated to the Atlantic. Jourdain et al. (2007), considering the vertical distribution, noted that there are actually “two maxima: one in the lower troposphere north of the ITCZ and one in the middle and upper troposphere south of the ITCZ”; this feature was, in fact, also observed during the Aerosols99 campaign. The studies overviewed here are nearly unanimous in their assessment that the ozone wave one and Atlantic paradox (when observed) are likely the product of three different sources: O_3 precursors from biomass burning and lightning, and stratosphere–troposphere exchange (STE), sometimes referred to as “stratospheric intrusions” (e.g., Pan et al. 2009).

TRANS-ATLANTIC RAOB CROSS SECTIONS: OZONE. The combined AEROSE campaign ozonesonde data have resulted in the most extensive in situ soundings of atmospheric ozone profiles over the tropical Atlantic ever attempted (see Table 1). Like the PTU soundings, the ozonesondes are of sufficient frequency to perform trans-Atlantic cross-sectional analyses.

Figures 14a–e shows the meridional cross sections for the AEROSE transects shown previously (Figs. 5, 11, and 12), with the ozone cross section from the Aerosols99 “baseline” (described in Thompson et al. 2000) shown in Fig. 14f for reference. Zonal cross sections are omitted because of page constraints. Generally speaking, AEROSE mid to high-level tropospheric ozone concentrations correlate with the dry layers (notably excluding SALs) seen in Figs. 11a–e. The 2008 RB-08-03 interhemispheric transect (Fig. 14a) is the most similar to Aerosols99 in terms of cruise track (Fig. 2), although AEROSE/RB-08-03 (Aerosols99) was during boreal spring (winter) and sampled the western (eastern) South Atlantic at lower

(higher) horizontal resolution. Most notable when comparing these two cross sections (Figs. 14a,f) is what appears to be a “reversal” in the midlevel tropospheric ozone (5–10 km), with the May 2008 data showing elevated O_3 in the NH, between 15° and 30°N, instead of the SH between 0° and 23°S, as in January 1999. The low-level (0–5 km) O_3 concentrations, on the other hand, show more similarity. The remaining AEROSE NH cross sections (Figs. 14b–e) are arranged in mean ordinal date order, and the two following the 2008 section (Figs. 14b,c), also during the month of May, show similar ozone concentrations and patterns to the 2008 NH data. The next two cross sections (Figs. 14d,e), spanning early to mid summer, show a trend toward increasing amounts of NH mid to upper tropospheric ozone. Furthermore, elevated mid to upper tropospheric NH O_3 is seen to span much of the tropical North Atlantic during these periods in the zonal cross sections (not shown). These observations thus seem to corroborate earlier observations of a NH O_3 maximum in JJA (e.g., Jenkins and Ryu 2004; Ziemke et al. 2006; Jenkins et al. 2008).

To provide some context on the 2008 measurements, Fig. 15 shows PATMOS-x AVHRR May 2008 mean $0.63 \mu\text{m } \tau_a$ and derived α , the May 2008 Moderate Resolution Imaging Spectroradiometer (MODIS) fire product [see Giglio et al. (2003) for more details on the MODIS fire product], and the ECMWF 860-hPa wind and total precipitable water (TPW) fields for 2–18 May. We note well-known regions of significant biomass burning typically occurring this time of year evident in the MODIS Fire Product (lower left plot), including African savannas between 0° and 20°S and 15° and 30°E as well as the Yucatan Peninsula. There are also some regions with less intense burning including the vicinity of Senegal as well as regions in South America, particularly Venezuela. The smoke emissions of these burning sites are clearly manifest in the PATMOS-x τ_a and α (top left and right, respectively), especially α .

Now considering the 2008 AEROSE transit data, the cruise track (Fig. 15, lower left) passes from a region of background marine aerosols with $\tau_a \approx 0.1$ south of the ITCZ to a region of increasing τ_a and α (starting around 9 May) north of it. This is seen in the AVHRR τ_a , α and ECMWF model TPW (Fig. 15 upper and lower right plots, respectively) as well as the Microtops measurements onboard the *Ronald H. Brown* (Fig. 5a). As mentioned above, the ship first passes through the main trans-Atlantic plume around 10°N. Following this peak, we see a gradual increase in τ_a from ≈ 0.1 to 0.2 with an attendant increase in Microtops α from ≈ 0.2 to 0.6, leading one to suspect

an increase in smaller-mode aerosols characteristic of smoke and/or industrial haze. NOAA HYSPLIT model 96-h back trajectories (not shown because of page constraints) ending at ozonesonde launches in the vicinity of 10°N confirm tropospheric parcels originating from Africa along the main dust plume axis, but for launches to the north of this at ~15°N the trajectories shift to origins out of the Caribbean Sea, the Gulf of Mexico, and North America. These observations are consistent with the hypothesis of tropospheric ozone formation from CO precursors present in smoke outflows possibly originating from biomass burning (e.g., from the Yucatan and Caribbean) or possibly anthropogenic smog from the U.S. east coast urban corridor. Regarding the lower concentrations of SH tropospheric O₃ seen in our data, especially as compared to Aerosols99, despite the significant savanna biomass burning in Africa (Fig. 15,

lower left) the smoke plume simply does not extend to the western Atlantic (Fig. 15, top plots), possibly being advected northward into the ITCZ within the monsoonal flow (cf. Jonquière et al. 1998). IR sounders (CrIS, IASI, AIRS) are capable of retrieving both O₃ and CO simultaneously—analyses of sounder trace-gas products, along with more focused studies on the AEROSE ozone measurements, both sonde and surface based, are to be the subjects of future work.

SUMMARY. This paper has provided an overview of the NOAA Aerosols and Ocean Science Expeditions (AEROSE), trans-Atlantic intensive campaigns begun in 2004 and conducted yearly since 2006 in collaboration with the PIRATA Northeast Extension (PNE) project. Science topics germane to the tropical Atlantic atmosphere were highlighted, particularly micro-, meso-, and synoptic-scale marine phenomena

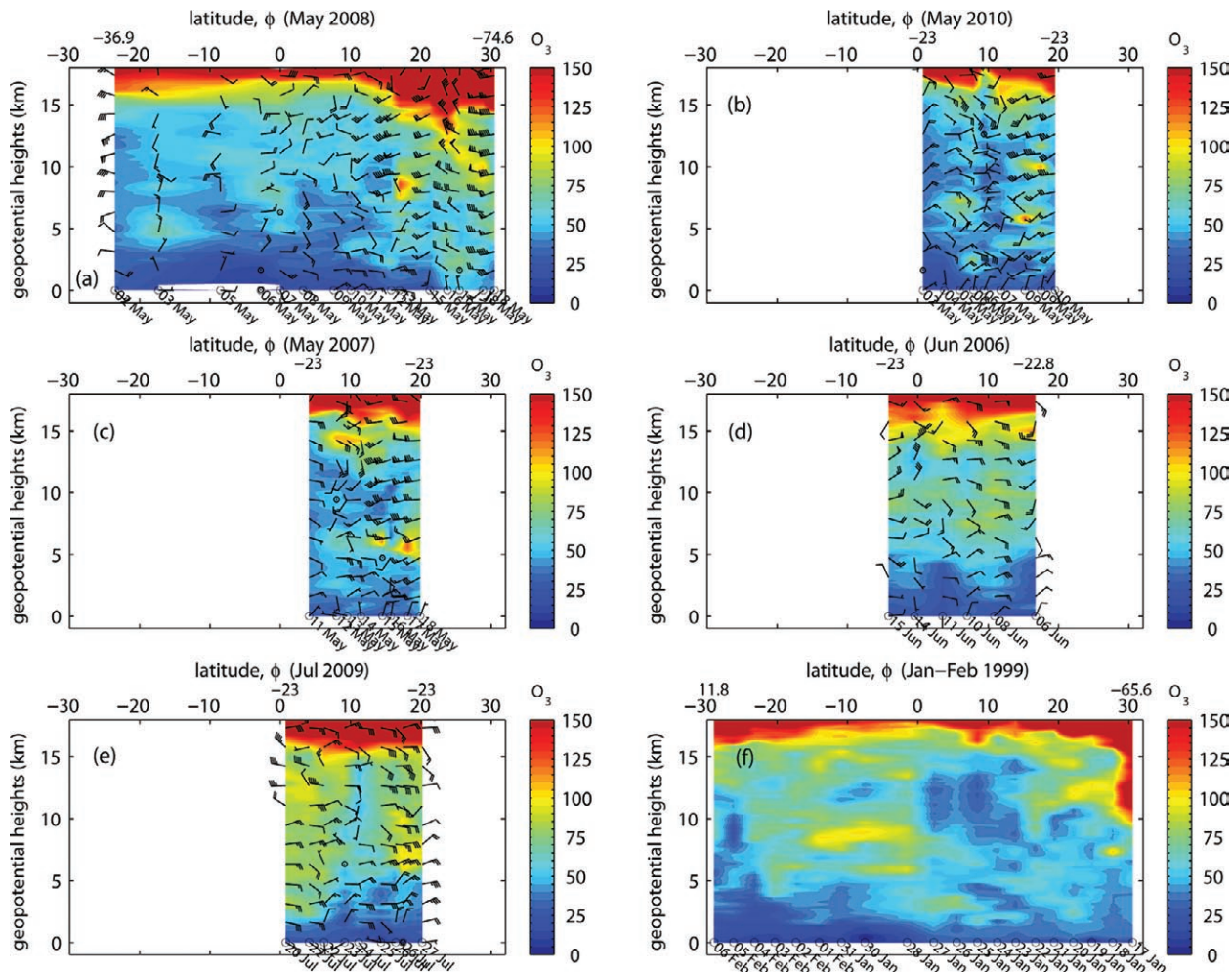


FIG. 14. As in Figs. 11 and 12, but showing cross-sectional contour analyses of ozonesonde O₃ measurements, with partial pressure converted to volumetric mixing ratio in ppbv using the concurrent RS92 PTU measurements, the lower right panel showing results from ozonesondes launched during the Aerosols99 cruise for comparison (cf. Thompson et al. 2000).

related to air mass outflows from Africa and other continental regions. It was noted that advanced environmental satellite observing systems both current (e.g., IASI/AMSU and AIRS/AMSU) and future (e.g., the JPSS CrIMSS and GOES-R ABI) are designed for the observation of such phenomena, thus requiring validation of EDR products under such conditions over open ocean. To this end, attention was given to a unique compilation of multiyear atmospheric in situ temperature, water vapor, wind, and ozone profiles derived from dedicated balloon-borne radiosondes launched to coincide with overpasses of the NASA A-Train *Aqua* and EUMETSAT MetOp satellites. The sonde launch frequencies during each campaign allow for unique multiyear zonal and meridional cross-sectional analyses of the tropical Atlantic, and as such are valuable for study of African dust and

smoke aerosol outflows, the associated SAL and distribution of tropical water vapor, and the dynamics of tropospheric ozone, as well as providing the correlative data necessary for satellite validation; more focused work pertaining to these topics will be the subject of future papers.

Fortuitously, NOAA has been committed to maintaining the PNE array, and has thus far supported yearly PNE/AEROSE cruises to this end, tentatively slated to continue through 2012. Campaigns beyond 2012 are less certain but would nevertheless contribute to the current unprecedented data complement and would also potentially provide the platform for acquiring open-ocean correlative data for the intensive calibration/validation phase of CrIMSS EDR products following the tentative launch of the NPP satellite in 2011.

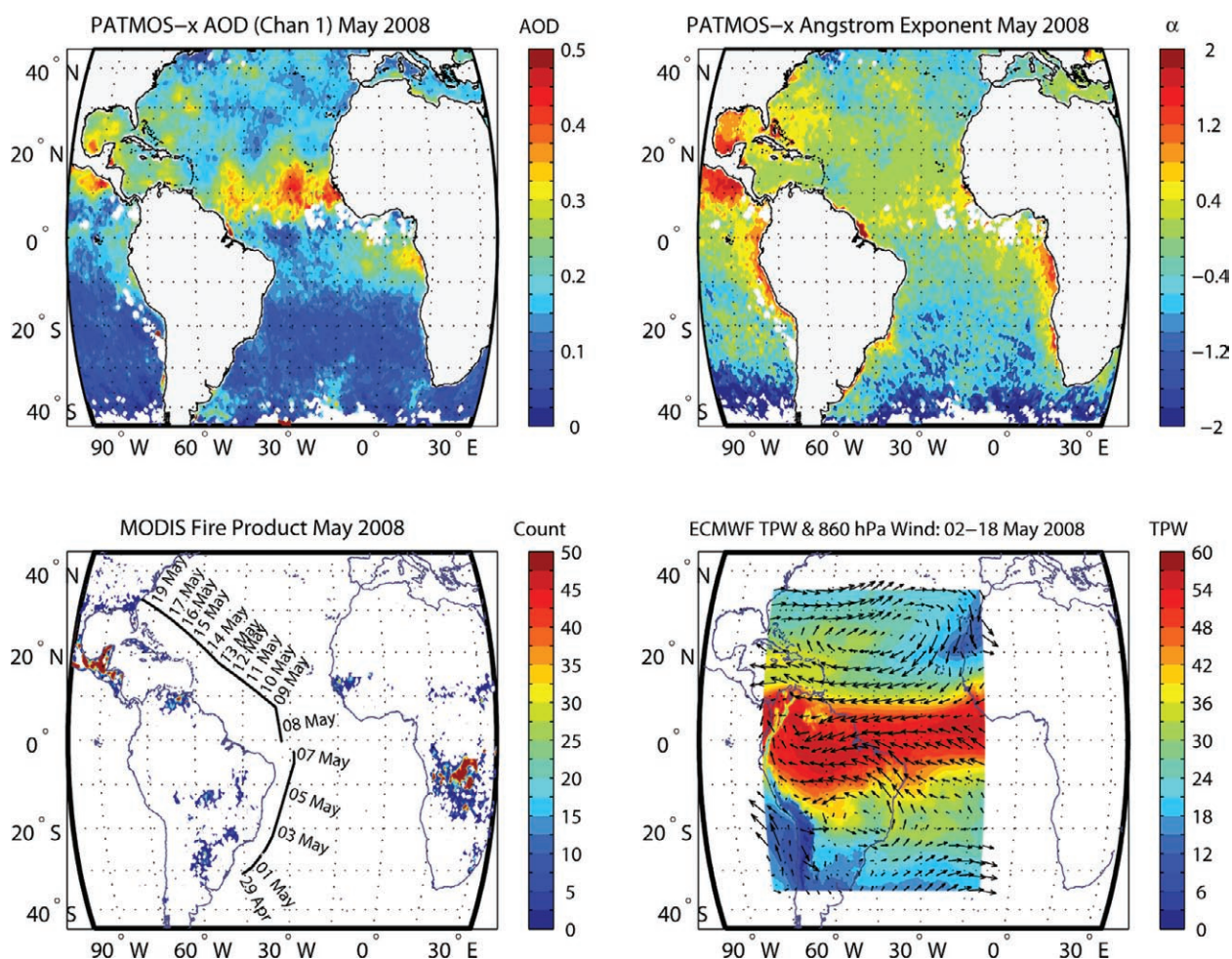


FIG. 15. Prevailing aerosol, fire, wind, and water vapor conditions during the AEROSE RB-08-03 interhemispheric transit (May 2008): (top left) PATMOS-x AVHRR mean channel 1 ($0.63 \mu\text{m}$) AOD, (top right) mean Angstrom exponent (α) derived from channels 1 and 2 ($0.63, 0.83 \mu\text{m}$), (bottom left) total fire counts from the MODIS CMG Fire Product (Giglio et al. 2003) (with RB-08-03 cruise track superimposed), and (bottom right) mean 860-hPa wind and TPW fields from the ECMWF model analysis (restricted to the AEROSE space-time domain, 2–18 May). Map projections are equal area.

ACKNOWLEDGMENTS. This research has been supported by the NOAA Educational Partnership Program Grant NA17AE1625, NOAA Grant NA17AE1623 to establish NCAS, the STAR Satellite Meteorology and Climatology Division (SMCD) and GOES-R Algorithm Working Group (M. D. Goldberg, SMCD Division Chief, and A. Powell, Director of STAR), the NOAA Integrated Program Office (2008–10), the Joint Center for Satellite Data Assimilation FY05–06 Science Development and Implementation Task, and the NASA AIRS Science Team (2006–08). Funding for PNE is provided by NOAA's Office of Climate Observations (Climate Program Office).

Predictions for LEO satellite overpasses were made possible via the orbit prediction utility developed by L. Nguyen and can be accessed at the NASA Langley Clouds and Radiation Group Web page (<http://www-angler.larc.nasa.gov>). The NOAA Air Resources Laboratory (ARL) is acknowledged for the provision of the HYSPLIT transport and dispersion model. The AVHRR PATMOS-x climate data were developed by A. Heidinger et al. (STAR, UW-Madison) and made available for download on the PATMOS-x project Web page (<http://cimss.ssec.wisc.edu/patmosx/>). The AMMA program is a French initiative built by an international scientific group and funded by a large number of agencies, especially from France, the United Kingdom, the United States, and Africa. SEVIRI multichannel and IASI hyperspectral data are obtained through a collaborative agreement between NOAA and EUMETSAT. NOAA-unique IASI retrieval products from the NESDIS/STAR IASI Operational Product Processing System are available on the NOAA CLASS Web site (www.nsof.class.noaa.gov/saa/products/welcome, search for IASI on pull-down menu).

We are grateful to numerous individuals who supported or contributed to AEROSE over the years: P. Clemente-Colón (National Ice Center), who was the Chief Scientist of AEROSE-I, and C. Schmid (NOAA/AOML), a PNE Chief Scientist; T. Zhu (CSU/CIRA) for SEVIRI data support; C. Dean (QSS/PSGS Program Manager); T. Pagano (JPL) and W. Feltz, R. Knuteson (UW/CIMSS) for sonde support; T. Schmit and J. Li (UW/CIMSS GOES-R Soundings Team); and G. Jenkins (Howard U.) for AMMA collaboration. Cruise participants who supported sonde operations include E. Roper (Lincoln U.) and R. Armstrong and Y. Detrés (UPRM). We also acknowledge the many students who assisted in and facilitated the collection data throughout the cruises (too numerous to list completely here), especially Howard University students A. Flores (Microtops and post-cruise data management), C. Stearns (ozonesonde prep and sonde inventory), M. Oyola, L. Roldán-Otero, and M. Hawkins; C. Spells (Hampton U.); and M. Guereque (UTEP). Finally, we extend our appreciation to all the crew and officers of the *Ronald H.*

Brown for their support throughout the years, as well as two anonymous reviewers for their helpful comments. The views, opinions, and findings contained in this paper are those of the authors and should not be construed as an official NOAA or U.S. Government position, policy, or decision.

REFERENCES

- Bates, T. S., and Coauthors, 2001: Regional physical and chemical properties of the marine boundary layer aerosol across the Atlantic during Aerosols99: An overview. *J. Geophys. Res.*, **106** (D18), 20 767–20 782.
- Bourlès, B., and Coauthors, 2008: The PIRATA program: History, accomplishments, and future directions. *Bull. Amer. Meteor. Soc.*, **89**, 1111–1125.
- Carlson, T. N., and J. M. Prospero, 1972: The large-scale movement of Saharan air outbreaks over the northern equatorial Atlantic. *J. Appl. Meteor.*, **11**, 283–297.
- Cayla, F. R., 1993: IASI infrared interferometer for operations and research. *High Spectral Resolution Infrared Remote Sensing for Earth's Weather and Climate Studies*, A. Chedin, M. T. Chahine, and N. A. Scott, Eds., NATO ASI Series I, Vol. 19, Springer-Verlag, 9–19.
- Chahine, M. T., and Coauthors, 2006: AIRS: Improving weather forecasting and providing new data on greenhouse gases. *Bull. Am. Meteor. Soc.*, **87**, 911–926.
- Dessler, A. E., and S. C. Sherwood, 2009: A matter of humidity. *Science*, **323**, 1020–1021.
- Dunion, J. P., and C. S. Velden, 2004: The impact of the Saharan air layer on Atlantic tropical cyclone activity. *Bull. Amer. Meteor. Soc.*, **85**, 353–385.
- , and C. S. Marron, 2008: A reexamination of the Jordan mean tropical sounding based on awareness of the Saharan air layer: Results from 2002. *J. Climate*, **21**, 5242–5253.
- Evan, A. T., J. Dunion, J. A. Foley, A. K. Heidinger, and C. S. Velden, 2006: New evidence for a relationship between Atlantic tropical cyclone activity and African dust outbreaks. *Geophys. Res. Lett.*, **33**, L19813, doi:10.1029/2006GL026408.
- Feltz, W. F., W. L. Smith, R. O. Knuteson, H. E. Revercomb, H. M. Woolf, and H. B. Howell, 1998: Meteorological applications of temperature and water vapor retrievals from the ground-based Atmospheric Emitted Radiance Interferometer (AERI). *J. Appl. Meteor.*, **37**, 857–875.
- Giglio, L., J. Desloîtres, C. O. Justice, and Y. J. Kaufman, 2003: An enhanced contextual fire detection

- algorithm for MODIS. *Remote Sens. Environ.*, **87**, 273–282.
- Hagan, D. E., and P. J. Minnett, 2003: AIRS radiance validation over ocean from sea surface temperature measurements. *IEEE Trans. Geosci. Remote Sensing*, **41**, 432–441.
- Hanafin, J. A., and P. J. Minnett, 2005: Measurements of the infrared emissivity of a wind-roughened sea surface. *Appl. Optics*, **44**, 398–411.
- Hobbs, P. V., 2000: *Introduction to Atmospheric Chemistry*. Cambridge University Press, 262 pp.
- Huang, H.-L., W. L. Smith, and H. M. Woolf, 1992: Vertical resolution and accuracy of atmospheric infrared sounding spectrometers. *J. Appl. Meteor.*, **31**, 265–274.
- Jacobowitz, H., L. L. Stowe, G. Ohring, A. Heidinger, K. Knapp, and N. R. Nalli, 2003: The advanced very high resolution radiometer Pathfinder Atmosphere (PATMOS) climate dataset: A resource for climate research. *Bull. Amer. Meteor. Soc.*, **84**, 785–793.
- Jenkins, G. S., and J. H. Ryu, 2004: Space-borne observations link the tropical Atlantic ozone maximum and paradox to lightning. *Atmos. Chem. Phys.*, **4**, 361–375.
- , M. Camara, and S. A. Nidaye, 2008: Observational evidence of enhanced middle/upper tropospheric ozone via convective processes over the equatorial tropical Atlantic during the summer of 2006. *Geophys. Res. Lett.*, **35**, L12806, doi:10.1029/2008GL033954.
- Jonquière, I., A. Marengo, A. Maalej, and F. Rohrer, 1998: Study of ozone formation and transatlantic transport from biomass burning emissions over West Africa during the airborne Tropospheric Ozone Campaigns TROPOZ I and TROPOZ II. *J. Geophys. Res.*, **103** (D15), 19 059–19 073.
- Jordan, C. L., 1958: Mean soundings for the West Indies area. *J. Meteor.*, **15**, 91–97.
- Jourdain, L., and Coauthors, 2007: Tropospheric vertical distribution of tropical Atlantic ozone observed by TES during the northern African biomass burning season. *Geophys. Res. Lett.*, **34**, L04810, doi:10.1029/2006GL028284.
- Kahn, R. A., and Coauthors, 2004: Aerosol data sources and their roles within PARAGON. *Bull. Amer. Meteor. Soc.*, **85**, 1511–1522.
- Karyampudi, V. M., and H. F. Pierce, 2002: Synoptic-scale influence of the Saharan air layer on tropical cyclogenesis over the eastern Atlantic. *Mon. Wea. Rev.*, **130**, 3100–3128.
- King, T., and Coauthors, 2008: The NOAA/NESDIS/STAR IASI operational product processing system. *Proc. 2008 EUMETSAT Meteorological Satellite Conf.*, Darmstadt, Germany, EUMETSAT.
- Le Marshall, J., and Coauthors, 2006: Improving global analysis and forecasting with AIRS. *Bull. Amer. Meteor. Soc.*, **87**, 891–894.
- Maddy, E. S., and C. D. Barnett, 2008: Vertical resolution estimates in version 5 of AIRS operational retrievals. *IEEE Trans. Geosci. Remote Sensing*, **46**, 2375–2384.
- Mapes, B. E., and P. Zuidema, 1996: Radiative-dynamical consequences of dry tongues in the tropical atmosphere. *J. Atmos. Sci.*, **53**, 620–638.
- Markowicz, K. M., P. J. Flatau, A. E. Kaldas, J. Remiszewska, K. Stelmazczyk, and L. Woeste, 2008: Ceilometer retrieval of the boundary layer vertical aerosol extinction structure. *J. Atmos. Oceanic Technol.*, **25**, 928–944.
- Minnett, P. J., R. O. Knuteson, F. A. Best, B. J. Osborne, J. A. Hanafin, and O. B. Brown, 2001: The Marine-Atmospheric Emitted Radiance Interferometer (M-AERI): A high-accuracy, sea-going infrared spectroradiometer. *J. Atmos. Oceanic Technol.*, **18**, 994–1013.
- Morris, V., and Coauthors, 2006: Measuring trans-Atlantic aerosol transport from Africa. *Eos, Trans. Amer. Geophys. Union*, **87**, 565–571.
- , T.-W. Yu, E. Joseph, R. Armstrong, R. Fitzgerald, R. Karim, X.-Z. Liang, and Q. Min, 2007: The NOAA Center for Atmospheric Sciences (NCAS): Programs and achievements. *Bull. Amer. Meteor. Soc.*, **88**, 141–145.
- , E. Joseph, S. Smith, and T.-W. Yu, 2010: The Howard University Program in Atmospheric Sciences (HUPAS): A program exemplifying diversity and opportunity. *J. Geosci. Educ.*, in press.
- Nalli, N. R., and L. L. Stowe, 2002: Aerosol correction for remotely sensed sea surface temperatures from the National Oceanic and Atmospheric Administration advanced very high resolution radiometer. *J. Geophys. Res.*, **107**, 3172, doi:10.1029/2001JC001162.
- , and Coauthors, 2005: Profile observations of the Saharan air layer during AEROSE 2004. *Geophys. Res. Lett.*, **32**, L05815, doi:10.1029/2004GL022028.
- , and Coauthors, 2006: Ship-based measurements for infrared sensor validation during Aerosol and Ocean Science Expedition 2004. *J. Geophys. Res.*, **111**, D09S04, doi:10.1029/2005JD006385.
- , P. J. Minnett, E. Maddy, W. W. McMillan, and M. D. Goldberg, 2008a: Emissivity and reflection model for calculating unpolarized isotropic water surface leaving radiance in the infrared. 2: Validation using Fourier transform spectrometers. *Appl. Optics*, **47**, 4649–4671.
- , H. Xie, C. D. Barnett, and M. D. Goldberg, 2008b: Using AEROSE-domain SEVIRI data

- for legacy sounding products from the GOES-R Advanced Baseline Imager. *Proc. 2008 EUMETSAT Meteorological Satellite Conf.*, Darmstadt, Germany, EUMETSAT.
- Pan, L. L., and Coauthors, 2009: Tropospheric intrusions associated with the secondary tropopause. *J. Geophys. Res.*, **114**, D10302, doi:10.1029/2008JD011374.
- Pierrehumbert, R. T., 1998: Lateral mixing as a source of subtropical water vapor. *Geophys. Res. Lett.*, **25**, 151–154.
- , and R. Roca, 1998: Evidence for control of Atlantic subtropical humidity by large scale advection. *Geophys. Res. Lett.*, **25**, 4537–4540.
- , H. Brogniez, and R. Roca, 2007: On the relative humidity of the atmosphere. *The Global Circulation of the Atmosphere*, Princeton University Press, 143–185.
- Prospero, J. M., R. A. Glaccum, and R. T. Nees, 1981: Atmospheric transport of soil dust from Africa to South America. *Nature*, **289**, 570–572.
- Redelsperger, J.-L., C. D. Thorncroft, A. Diedhiou, T. Lebel, D. J. Parker, and J. Polcher, 2006: African Monsoon Multidisciplinary Analysis: An international research project and field campaign. *Bull. Amer. Meteor. Soc.*, **87**, 1739–1746.
- Resch, F., A. Sunnu, and G. Afeti, 2008: Saharan dust flux and deposition rate near the Gulf of Guinea. *Tellus*, **60B**, 98–105.
- Robinson, L., J. Rousseau, D. Mapp, V. Morris, and M. Laster, 2007: An educational partnership program with minority serving institutions: A framework for producing minority scientists in NOAA-related disciplines. *J. Geosci. Educ.*, **55**, 486–492.
- Sauvage, B., V. Thouret, A. M. Thompson, J. C. Witte, J.-P. Cammas, P. Nédélec, and G. Athier, 2006: Enhanced view of the “tropical Atlantic ozone paradox” and “zonal wave one” from the in situ MOZAIC and SHADOZ data. *J. Geophys. Res.*, **111**, D01301, doi:10.1029/2005JD006241.
- Schmetz, J., P. Pili, S. Tjemkes, D. Just, J. Kerkmann, S. Rota, and A. Ratier, 2002: An introduction to Meteosat Second Generation (MSG). *Bull. Amer. Meteor. Soc.*, **83**, 977–992.
- Schmit, T. J., M. M. Gunshor, W. P. Menzel, J. J. Gurka, J. Li, and A. S. Bachmeier, 2005: Introducing the next-generation advanced baseline imager on GOES-R. *Bull. Amer. Meteor. Soc.*, **86**, 1079–1096.
- Sherwood, S. C., E. R. Kursinski, and W. G. Read, 2006: A distribution law for free-tropospheric relative humidity. *J. Climate*, **19**, 6267–6277.
- Smirnov, A., and Coauthors, 2009: Maritime Aerosol Network as a component of Aerosol Robotic Network. *J. Geophys. Res.*, **114**, D06204, doi:10.1029/2008JD011257.
- Smith, W. L., and Coauthors, 1996: Observations of the infrared properties of the ocean: Implications for the measurement of sea surface temperature via satellite remote sensing. *Bull. Amer. Meteor. Soc.*, **77**, 41–51.
- Stowe, L. L., and H. E. Fleming, 1980: The error in satellite retrieved temperature profiles due to the effects of atmospheric aerosol particles. *Remote Sens. Environ.*, **9**, 57–64.
- Stull, R. B., 1991: Static stability—An update. *Bull. Amer. Meteor. Soc.*, **72**, 1521–1529.
- Sun, D., K. M. Lau, and M. Kafatos, 2008: Contrasting the 2007 and 2005 hurricane seasons: Evidence of possible impacts of Saharan dry air and dust on tropical cyclone activity in the Atlantic basin. *Geophys. Res. Lett.*, **35**, L15405, doi:10.1029/2008GL034529.
- Szczodrak, M., P. J. Minnett, N. R. Nalli, and W. F. Feltz, 2007: Profiling the lower troposphere over the ocean with infrared hyperspectral measurements of the Marine-Atmosphere Emitted Radiance Interferometer. *J. Atmos. Oceanic Technol.*, **34**, 390–402.
- Thompson, A. M., and Coauthors, 2000: A tropical Atlantic paradox: Shipboard and satellite views of a tropospheric ozone maximum and wave-one in January–February 1999. *Geophys. Res. Lett.*, **27**, 3317–3320.
- , and Coauthors, 2003: Southern Hemisphere Additional Ozonesondes (SHADOZ) 1998–2000 tropical ozone climatology. 2. Tropospheric variability and the zonal wave-one. *J. Geophys. Res.*, **108**, 8241, doi:10.1029/2002JD002241.
- Voss, K. J., E. J. Welton, P. K. Quinn, R. Frouin, M. Miller, and R. M. Reynolds, 2001: Aerosol optical depth measurements during the Aerosols99 experiment. *J. Geophys. Res.*, **106** (D18), 20 811–20 819.
- Weaver, C. J., J. Joiner, and P. Ginoux, 2003: Mineral aerosol contamination of TIROS Operational Vertical Sounder (TOVS) temperature and moisture retrievals. *J. Geophys. Res.*, **108**, 4246, doi:10.1029/2002JD002571.
- Wong, S., and A. E. Dessler, 2005: Suppressing of deep convection over the tropical North Atlantic by the Saharan air layer. *Geophys. Res. Lett.*, **32**, L09808, doi:10.1029/2004GL022295.
- , —, N. M. Mahowald, P. Yang, and Q. Feng, 2009: Maintenance of lower tropospheric temperature inversion in the Saharan air layer by dust and dry anomaly. *J. Climate*, **22**, 5149–5162.
- Wu, L., 2007: Impact of Saharan air layer on hurricane peak intensity. *Geophys. Res. Lett.*, **34**, L09802, doi:10.1029/2007GL029564.
- , 2009: Comparison of atmospheric infrared sounder temperature and relative humidity profiles with

- NASA African Monsoon Multidisciplinary Analysis (NAMMA) dropsonde observations. *J. Geophys. Res.*, **114**, D19205, doi:10.1029/2009JD012083.
- Zhang, C., and J. Pennington, 2004: African dry air outbreaks. *J. Geophys. Res.*, **109**, D20108, doi:10.1029/2003JD003978.
- Zhang, J., and Q. Zhang, 2008: Aerosol impact and correction on temperature profile retrieval from MODIS. *Geophys. Res. Lett.*, **35**, L13818, doi:10.1029/2008GL034419.
- Zhao, X.-P., I. Laszlo, W. Guo, A. Heidinger, C. Cao, A. Jelenak, D. Tarpley, and J. Sullivan, 2008: Study of long-term trend in aerosol optical thickness observed from operational AVHRR satellite instrument. *J. Geophys. Res.*, **113**, D07201, doi:10.1029/2007JD009061.
- Ziemke, J. R., S. Chandra, B. N. Duncan, L. Froidevaux, P. K. Bhartia, P. F. Levelt, and J. W. Waters, 2006: Tropospheric ozone determined from Aura OMI and MLS: Evaluation of measurements and comparison with the Global Modeling Initiatives Chemical Transport Model. *J. Geophys. Res.*, **111**, D19303, doi:10.1029/2006JD007089.
- Zipser, E. J., and Coauthors, 2009: The Saharan air layer and the fate of African easterly waves: NASA's AMMA field study of tropical cyclogenesis. *Bull. Amer. Meteor. Soc.*, **90**, 1137–1156.